(12) INTERNATIONAL APPLICATION PUBLISHED UNDER THE PATENT COOPERATION TREATY (PCT)

(19) World Intellectual Property Organization
International Bureau

(43) International Publication Date
19 December 2002 (19.12.2002)

PCT

(10) International Publication Number
WO 02/101838 A1

(51) International Patent Classification[7]: H01L 31/0256, 31/04, 31/06

(21) International Application Number: PCT/US02/18183

(22) International Filing Date: 7 June 2002 (07.06.2002)

(25) Filing Language: English

(26) Publication Language: English

(30) Priority Data:
09/878,523 11 June 2001 (11.06.2001) US
09/948,226 6 September 2001 (06.09.2001) US

(71) Applicant: THE TRUSTEES OF PRINCETON UNIVERSITY [US/US]; P.O. Box 36, Princeton, NJ 08544-0036 (US).

(72) Inventors: FORREST, Stephen, R.; 148 Hunt Drive, Princeton, NJ 08540 (US). PEUMANS, Peter; Graduate College, Princeton University, Princeton, NJ 08544 (US). YAKIMOV, Aharon; 34-06 Quail Ridge Drive, Plainsboro, NJ 08536 (US).

(74) Agents: MEAGHER, Thomas, F. et al.; Kenyon & Kenyon, One Broadway, New York, NY 10004 (US).

(81) Designated States *(national)*: AE, AG, AL, AM, AT, AU, AZ, BA, BB, BG, BR, BY, BZ, CA, CH, CN, CO, CR, CU, CZ, DE, DK, DM, DZ, EC, EE, ES, FI, GB, GD, GE, GH, GM, HR, HU, ID, IL, IN, IS, JP, KE, KG, KP, KR, KZ, LC, LK, LR, LS, LT, LU, LV, MA, MD, MG, MK, MN, MW, MX, MZ, NO, NZ, OM, PH, PL, PT, RO, RU, SD, SE, SG, SI, SK, SL, TJ, TM, TN, TR, TT, TZ, UA, UG, UZ, VN, YU, ZA, ZM, ZW.

(84) Designated States *(regional)*: ARIPO patent (GH, GM, KE, LS, MW, MZ, SD, SL, SZ, TZ, UG, ZM, ZW), Eurasian patent (AM, AZ, BY, KG, KZ, MD, RU, TJ, TM), European patent (AT, BE, CH, CY, DE, DK, ES, FI, FR, GB, GR, IE, IT, LU, MC, NL, PT, SE, TR), OAPI patent (BF, BJ, CF, CG, CI, CM, GA, GN, GQ, GW, ML, MR, NE, SN, TD, TG).

Published:
— *with international search report*

For two-letter codes and other abbreviations, refer to the "Guidance Notes on Codes and Abbreviations" appearing at the beginning of each regular issue of the PCT Gazette.

WO 02/101838 A1

(54) Title: ORGANIC PHOTOVOLTAIC DEVICES

(57) Abstract: The present invention generally relates to organic photosensitive optoelectronic devices. More specifically, it is directed to organic photovoltaic devices, e.g., organic solar cells. Further, it is directed to an optimized organic solar cell comprising multiple stacked subcells in series. High power conversion efficiency are achieved by fabrication of a photovoltaic cell comprising multiple stacked subcells with thickness optimization and employing an electron blocking layer.

ORGANIC PHOTOVOLTAIC DEVICES

FIELD OF INVENTION

The present invention generally relates to organic photosensitive optoelectronic devices. More specifically, it is directed to organic photovoltaic devices, e.g., organic solar cells. Further, it is directed to an optimized organic solar cell with greatly improved efficiency. Improved efficiency is achieved through improved materials choice, device configuration and/or device processing technique.

BACKGROUND OF THE INVENTION

Optoelectronic devices rely on the optical and electronic properties of materials to either produce or detect electromagnetic radiation or to generate electricity from ambient electromagnetic radiation. Photosensitive optoelectronic devices convert electromagnetic radiation into electricity. Solar cells, also known as photovoltaic (PV) devices, are used to generate electrical power from ambient light. PV devices are used to drive power consuming loads to provide, for example, lighting, heating, or to operate electronic equipment such as computers or remote monitoring or communications equipment. These power generation applications often involve the charging of batteries or other energy storage devices so that equipment operation may continue when direct illumination from the sun or other ambient light sources is not available. As used herein, the term "resistive load" refers to any power consuming or storing device, equipment or system.

Traditionally, photosensitive optoelectronic devices have been constructed of a number of inorganic semiconductors, e.g., crystalline, polycrystalline and amorphous silicon, gallium arsenide, cadmium telluride and others. Herein the term "semiconductor" denotes materials which can conduct electricity when charge carriers are induced by thermal or electromagnetic excitation. The term "photoconductive" generally relates to the process in which electromagnetic radiant energy is absorbed and thereby converted to excitation energy of electric charge carriers so that the carriers

can conduct, i.e., transport, electric charge in a material. The terms "photoconductor" and "photoconductive material" are used herein to refer to semiconductor materials which are chosen for their property of absorbing electromagnetic radiation to generate electric charge carriers.

Solar cells are characterized by the efficiency with which they can convert incident solar power to useful electric power. Devices utilizing crystalline or amorphous silicon dominate commercial applications, and some have achieved efficiencies of 23% or greater. However, efficient crystalline-based devices, especially of large surface area, are difficult and expensive to produce due to the problems inherent in producing large crystals without significant efficiency-degrading defects. On the other hand, high efficiency amorphous silicon devices still suffer from problems with stability. Present commercially available amorphous silicon cells have stabilized efficiencies between 4 and 8%. More recent efforts have focused on the use of organic photovoltaic cells to achieve acceptable photovoltaic conversion efficiencies with economical production costs.

PV devices produce a photo-generated voltage when they are connected across a load and are irradiated by light. When irradiated without any external electronic load, a PV device generates its maximum possible voltage, V open-circuit, or V_{OC}. If a PV device is irradiated with its electrical contacts shorted, a maximum short-circuit current, or I_{SC}, is produced. When actually used to generate power, a PV device is connected to a finite resistive load and the power output is given by the product of the current and voltage, $I \times V$. The maximum total power generated by a PV device is inherently incapable of exceeding the product, $I_{SC} \times V_{OC}$. When the load value is optimized for maximum power extraction, the current and voltage have values, I_{max} and V_{max}, respectively.

A figure of merit for solar cells is the fill factor, *ff*, defined as:

$$ff = \frac{I_{max} V_{max}}{I_{SC} V_{OC}} \qquad (1)$$

where *ff* is always less than 1, as I_{SC} and V_{OC} are never obtained simultaneously in actual use.

Nonetheless, as *ff* approaches 1, the device is more efficient.

When electromagnetic radiation of an appropriate energy is incident upon a semiconductive organic material, for example, an organic molecular crystal (OMC) material, or a polymer, a photon can be absorbed to produce an excited molecular state. This is represented symbolically as $S_0 + h\nu \Rightarrow S_0^*$. Here S_0 and S_0^* denote ground and excited molecular states, respectively. This energy absorption is associated with the promotion of an electron from a bound state in the HOMO, which may be a π-bond, to the LUMO, which may be a π^*-bond, or equivalently, the promotion of a hole from the LUMO to the HOMO. In organic thin-film photoconductors, the generated molecular state is generally believed to be an exciton, i.e., an electron-hole pair in a bound state which is transported as a quasi-particle. The excitons can have an appreciable life-time before geminate recombination, which refers to the process of the original electron and hole recombining with each other, as opposed to recombination with holes or electrons from other pairs. To produce a photocurrent the electron-hole pair must become separated, typically at a donor-acceptor interface between two dissimilar contacting organic thin films. If the charges do not separate, they can recombine in a geminant recombination process, also known as quenching, either radiatively, by the emission of light of a lower energy than the incident light, or non-radiatively, by the production of heat. Either of these outcomes is undesirable in a photosensitive optoelectronic device.

Electric fields or inhomogeneities at a contact may cause an exciton to quench rather than dissociate at the donor-acceptor interface, resulting in no net contribution to the current. Therefore, it is desirable to keep photogenerated excitons away from the contacts. This has the effect of limiting the diffusion of excitons to the region near the junction so that the associated electric field has an increased opportunity to separate charge carriers liberated by the dissociation of the excitons near the junction.

To produce internally generated electric fields which occupy a substantial volume, the usual method is to juxtapose two layers of material with appropriately selected conductive properties, especially with respect to their distribution of molecular quantum energy states. The interface of these two materials is called a photovoltaic heterojunction. In traditional semiconductor theory,

materials for forming PV heterojunctions have been denoted as generally being of either n, or donor, type or p, or acceptor, type. Here n-type denotes that the majority carrier type is the electron. This could be viewed as the material having many electrons in relatively free energy states. The p-type denotes that the majority carrier type is the hole. Such material has many holes in relatively free energy states. The type of the background, i.e., not photo-generated, majority carrier concentration depends primarily on unintentional doping by defects or impurities. The type and concentration of impurities determine the value of the Fermi energy, or level, within the gap between the highest occupied molecular orbital (HOMO) and the lowest unoccupied molecular orbital (LUMO), called the HOMO-LUMO gap. The Fermi energy characterizes the statistical occupation of molecular quantum energy states denoted by the value of energy for which the probability of occupation is equal to ½. A Fermi energy near the LUMO energy indicates that electrons are the predominant carrier. A Fermi energy near the HOMO energy indicates that holes are the predominant carrier. Accordingly, the Fermi energy is a primary characterizing property of traditional semiconductors and the prototypical PV heterojunction has traditionally been the p-n interface.

The term "rectifying" denotes, inter alia, that an interface has an asymmetric conduction characteristic, i.e., the interface supports electronic charge transport preferably in one direction. Rectification is associated normally with a built-in electric field which occurs at the heterojunction between appropriately selected materials.

A significant property in organic semiconductors is carrier mobility. Mobility measures the ease with which a charge carrier can move through a conducting material in response to an electric field. As opposed to free carrier concentrations, carrier mobility is determined in large part by intrinsic properties of the organic material such as crystal symmetry and periodicity. Appropriate symmetry and periodicity can produce higher quantum wavefunction overlap of HOMO levels producing higher hole mobility, or similarly, higher overlap of LUMO levels to produce higher electron mobility. Moreover, the donor or acceptor nature of an organic semiconductor, e.g., 3,4,9,10-perylenetetracarboxylic dianhydride (PTCDA), may be at odds with the higher carrier mobility. For example, while chemistry arguments suggest a donor, or n-type, character for

PTCDA, experiments indicate that hole mobilities exceed electron mobilities by several orders of magnitude so that the hole mobility is a critical factor. The result is that device configuration predictions from donor/acceptor criteria may not be borne out by actual device performance. Due to these unique electronic properties of organic materials, rather than designating them as "p-type" or "acceptor-type" and "n-type" or "donor-type", the nomenclature of "hole-transporting-layer" (HTL) or "electron-transporting-layer" (ETL) is frequently used. In this designation scheme, an ETL will be preferentially electron conducting and an HTL will be preferentially hole transporting.

A typical prior art photovoltaic device configuration is the organic bilayer cell. In the bilayer cell, charge separation predominantly occurs at the organic heterojunction. The built-in potential is determined by the HOMO-LUMO energy difference between the two materials contacting to form the heterojunction. The HOMO-LUMO gap offset between the HTL and ETL produce an electric field around the HTL/ETL interface.

Organic PV cells have many potential advantages when compared to traditional silicon-based devices. Organic PV cells are light weight, economical in materials use, and can be deposited on low cost substrates, such as flexible plastic foils. However, organic PV devices typically have relatively low quantum yield (the ratio of photons absorbed to carrier pairs generated, or electromagnetic radiation to electricity conversion efficiency), being on the order of 1 % or less. This is, in part, thought to be due to the second order nature of the intrinsic photoconductive process. That is, carrier generation requires exciton generation, diffusion and ionization. However, the diffusion length (L_D) of an exciton is typically much less (L_D ~ 50Å) than the optical absorption length (~500Å), requiring a trade off between using a thick, and therefore resistive, cell with multiple or highly folded interfaces, or a thin cell with a low optical absorption efficiency. Different approaches to increase the efficiency have been demonstrated, including use of doped organic single crystals, conjugated polymer blends, and use of materials with increased exciton diffusion length. The problem was attacked yet from another direction, namely employment of different cell geometry, such as three-layered cell, having an additional mixed layer of co-deposited p- and n-type pigments, or fabricating tandem cell.

As was shown in previous work, the open circuit voltage (V_{OC}) of the tandem cell can be almost two times higher than that of the single cell. M. Hiramoto, M. Suezaki, and M. Yokoyama, *Chemistry Letters*, 327 (1990). Unfortunately, the obtained power conversion efficiency was less than for the single cell. That was attributed to the fact that the front cell attenuates light intensity coming to the back cell. Therefore the photocurrent produced by the back cell is reduced, thus limiting the power conversion efficiency. Additional reasoning was that doubling of the overall thickness in tandem devices results in increased series resistance, that also could affect the power conversion efficiency.

In order to increase the cell performance, materials and device configurations are desirable which can enhance the quantum yield and, therefore, the power conversion efficiency. We have now achieved high power conversion efficiency by fabrication of a photovoltaic cell comprising multiple stacked subcells with thickness optimization and employing an electron blocking layer. According to the present invention, improved materials choice, device configuration and device processing techniques allow for the construction of organic PV cells with power conversion efficiencies in excess of 4%.

SUMMARY AND OBJECTS OF INVENTION

The present invention provides organic-based photosensitive optoelectronic devices with greatly improved efficiency. Improved efficiency is achieved through improved materials choice, device configuration and/or device processing techniques.

The invention provides organic-based photosensitive optoelectronic devices that comprise materials that are selected to promote device efficiecy. It is an object of the ivnvention to provide devices with increased efficiency comprising an anode layer, a hole transporting (donor-type) layer, an electron transporting (acceptor-type) layer, and a cathode. A fullerene compound is a preferred material for use in the ETL in the devices of the present invention.

The invention also provides organic-based photosensitive optoelectronic devices that comprise a configuration that improves device efficiency. It is an object of the present invention to

provide an organic PV device with multiple stacked subcells in series between an anode layer and a cathode. Each subcell comprises an electron donor layer, and an electron acceptor layer in contact with the electron donor layer. The subcells are separated by an electron-hole recombination zone. Advantageously, the device also includes one or more exciton blocking layers (EBL) and a cathode smoothing layer.

It is an object of the present invention to provide an organic PV device with improved photovoltaic performance. To this end, the invention provides an organic PV device capable of operating with a high external quantum efficiency.

Another object of the present invention is to provide organic photosensitive optoelectronic devices with improved absorption of incident radiation for more efficient photogeneration of charge carriers.

It is a further objective of the present invention to provide organic photosensitive optoelectronic devices with an improved V_{OC} and an improved I_{SC}.

BRIEF DESCRIPTION OF THE DRAWINGS

The foregoing and other features of the present invention will be more readily apparent from the following detailed description of exemplary embodiments taken in conjunction with the attached drawings.

Figure 1 depicts a tandem (consisting of two subcells) device. Each subcell comprises a copper phthalocyanine (CuPc) / 3,4,9,10-perylenetetracarboxylic-bis-benzimidazole (PTCBI) heterojunction. The two subcells of the tandem device are separated by a thin layer of silver. Between the back subcell and the Ag cathode is depicted an electron blocking layer consisting of BCP.

Figure 2 illustrates the proposed energy level diagram of a tandem device as depicted in Figure 1. The operation of this cell is as follows: a photon is absorbed in one of the two subcells,

generating an exciton, which can diffuse in the organic films. CuPc/PTCBI interfaces provide an active site for the exciton dissociation. Upon dissociation of the light-generated excitons at the CuPc/PTCBI interfaces, the holes (open circles) are transported in the CuPc layers, while the electrons (filed circles) are transported in the PTCBI layers. Holes, which are generated in the front cell are collected by the ITO electrode. Electrons, which are generated in the back cell are collected by the Ag cathode. Holes from the back cell and electrons from the front cell are transported towards the Ag layer between the subcells, where they recombine.

Figure 3 shows the I-V characteristics (current density vs. voltage) of a tandem device before optimization (open squares) and a single cell device (filled squares) under 1 sun illumination. The cell structures are as follows: substrate/300Å CuPc/300Å PTCBI/20Å Ag/300Å CuPc/300Å PTCBI/800Å Ag - for tandem device, and substrate/300Å CuPc/300Å PTCBI/800Å Ag for the single cell device.

Figure 4 shows the short circuit current density (left axis) and open circuit voltage (right axis) for tandem cells, having front cells of different thicknesses. The measurements are performed under 1 sun illumination. Note both I_{SC} and V_{OC} have a maximum around 220 Å front cell thickness. This corresponds to the front cell structure: 110Å CuPc/110Å PTCBI. For devices with the thickness of the front cell larger than 220 Å, I_{SC} decreases due to increased optical absorption in the front cell, which leads to lower light intensity at the back cell, which limits the device current. For thicknesses smaller than 220 Å, I_{SC} decreases due to substrate roughness, as well as island formation in the organic layers.

Figure 5 shows a comparison of the I-V characteristics of two tandem cells: one with a BCP layer (filled squares) and another without (open squares). The BCP layer is incorporated in the back cell. The measurement is performed at 1 sun illumination. A significant increase of the photocurrent density can be clearly seen for the tandem cell having a BCP layer, thus confirming the usefulness of the EBL concept to tandem PV cells.

Figure 6 shows the Ag layer thickness dependence of the short circuit current density (I_{SC})

and the open circuit voltage (V_{OC}) produced by a tandem cell under AM 1.5 1 sun illumination. While the V_{OC} remains constant, the I_{SC} increases considerably upon decrease of the Ag layer thickness, and reaches its maximum value at the minimum Ag layer thickness deposited (5Å). V_{OC} and I_{SC} show significant drop for the device without an Ag layer. The observed dependence of the cell performance on the thickness of the Ag interlayer indicates that even a very small amount of Ag inserted between the front and the back subcells is enough to provide recombination sites at the interface between them.

Figure 7 shows the BCP layer thickness dependence of the short circuit current density (I_{SC}) and the open circuit voltage (V_{OC}) produced by a tandem cell under AM 1.5, 1 sun illumination. While the V_{OC} remains fairly constant, the I_{SC} shows a dependance on the BCP layer thickness, and reaches its maximum value at the BCP layer thickness of about 100 to 120 Å. V_{OC} and I_{SC} show significant drop for the device without BCP layer.

Figure 8 shows the forth quardrant of the I-V characteristics of an optimized tandem cell: ITO/PEDOT/110Å CuPc/110Å PTCBI/5Å Ag/150Å CuPc/250Å PTCBI/800Å Ag for different incident power densities for an AM 1.5 simulated solar spectrum. Approximately 100mW/cm^2 corresponds to 1 sun intensity.

Figure 9 shows the I-V characteristics of the optimized tandem cell: ITO/PEDOT/110Å CuPc/110Å PTCBI/5Å Ag/150Å CuPc/250Å PTCBI/800Å Ag measured at different incident light intensities. Power conversion efficiency of this optimized tandem device reaches its maximum of about 2.5% at light intensity of 0.5 sun.

Figure 10 illustrates the proposed energy diagram of the devices with ITO and PEDOT:PSS anodes. The Fermi level energies for the electrodes (ITO, PEDOT:PSS, and Al), and HOMO and LUMO levels for CuPc, C_{60}, and BCP are indicated. The ITO and PEDOT:PSS work function data are taken from T.M. Brown et al, *Appl. Phys. Lett.* **75,** 1679 (1999). The C_{60} ionization potential and electron affinity are taken from R. Mitsumoto et al. *J. Phys. Chem. A* **102,** 552 (1998), and I.G. Hill et al., *J. Appl. Phys.* **86,** 4515 (1999) was used for CuPc and BCP.

The electrode work functions and HOMO levels were obtained by ultraviolet photoelectron spectroscopy, and have error bars of ±0.1eV. The LUMO levels were estimated from the HOMO levels and the optical energy gap.

Figure 11 (upper panel) shows the plot of current density vs. voltage for the devices anode/200Å CuPc/200Å C_{60}/150Å BCP/800Å Al, where the anode is either ITO (cell A, squares), or ITO/PEDOT:PSS (cell B, circles). The open symbols represent I-V curves taken in the dark, while the filled symbols represent I-V curves taken under AM1.5G illumination with an intensity of 100mW/cm^2. The lower panel shows the plot of photocurrent density vs. voltage for the same devices (cell A: crossed squares, cell B: crossed circles). The photocurrent is the difference between the I-V curves taken in the dark and under illumination. Also shown is the photocurrent of cell A shifted by DV=+0.50V (cell A*, dashed line), which overlaps with the photocurrent curve of cell B.

Figure 12 shows the current-voltage characteristics of ITO/PEDOT:PSS/50Å CuPc/200Å C_{60}/100Å BCP/800Å Al devices under AM1.5G illumination of 100mW/cm$_2$. The PEDOT:PSS film was either untreated (filled squares), treated with an oxygen plasma (10W, 100mTorr, 30s: open squares), or treated with an Ar plasma (10W, 100mTorr, 30s: open circles). The inset shows the short circuit current of ITO/PEDOT:PSS/200Å CuPc/400Å C_{60}/BCP/800Å Al devices under AM1.5G illumination with an intensity of 100mW/cm^2, as a function of the thickness of the BCP layer. The smooth curve through the data points (open squares) is a guide to the eye.

Figure 13 shows the current-voltage characteristics of the optimized device structure: ITO/PEDOT:PSS(Ar treated)/200Å CuPc/400Å C_{60}/120Å BCP/1000Å Al under AM1.5G illumination of variable intensity. The maximum power output is indicated for illumination intensities of >150mW/cm^2, illustrating the effect of the series resistance on the *ff*.

Figure 14(a) shows the η_P, *ff* and V_{OC} of the optimized device with layer structure: ITO/PEDOT:PSS(Ar treated)/200Å CuPc/400Å C_{60}/120Å BCP/1000Å Al as a function of the incident optical power. Figure 14(b) shows the external quantum efficiency of the same device as a

function of wavelength. The photon flux corresponding to an AM1.5G solar spectrum is also shown for comparison.

DETAILED DESCRIPTION

The present invention provides organic-based photosensitive optoelectronic devices with greatly improved efficiency. Improved efficiency is achieved through improved materials choice, device configuration and/or device processing techniques.

The invention provides organic PV devices with increased efficiency comprising an anode layer, a hole transporting (donor-type) layer, an electron transporting (acceptor-type) layer, and a cathode. Through improved materials choice, devices may be fabricated that have increased efficiency. In one embodimsnt of the present invention, the ETL comprises a fullerene compound. Advantageously, the device also includes one or more exciton blocking layers (EBLs). Further, the device may also include a charge transfer layer.

The present invention also provides device configurations that yield improved device efficiency. In one ebodiment, the present invention provides stacked organic photosensitive optoelectronic devices comprised of multiple subcells. Each subcell comprises a donor- acceptor heterojunction. The subcells are separated by an electron-hole recombination zone. In preferred embodiments of the present invention, the electron-hole recombination zone comprises an ultra-thin metal layer which may be discontinuous. The devices of the present invention may comprise one or more subcells. Preferably, the devices will be comprised of two to five subcells. The organic photoconductive layers may be fabricated using vacuum deposition, spin coating, organic vapor-phase deposition, inkjet printing and other methods known in the art.

The high bulk resistivities of organic photoconductors make it desirable to utilize relatively thin films of these materials. However, thin photosensitive layers will absorb a smaller fraction of incident radiation, and thus the external quantum efficiency of thin-layer photoconductors may be lower than that of thick-layer photoconductors. The external quantum efficiency of thin-layer organic devices such as those described herein can be further enhanced, however, by a suitable

design of the device geometry. Due to the thin photoactive layers, device geometries which provide a means for increasing the effective thickness of the absorbant layers may be preferable. One such configuration is a stacked device as described in U.S. Patent Nos. 6,198,091, 6,198,092, and co-pending application serial number 09/136,377, incorporated herein by reference. As used herein, the terms "stack", "stacked", "multisection" and "multicell" refer to any optoelectronic device with multiple layers of a photoconductive material separated by one or more electrode or charge transfer layers. When the term "subcell" is used hereafter, it refers to an organic photosensitive optoelectronic construction. When a subcell is used individually as a photosensitive optoelectronic device, it typically includes a complete set of electrodes, i.e., positive and negative. As disclosed herein, in some stacked configurations it is possible for adjacent subcells to utilize common, i.e., shared, electrode or charge transfer layers. In other cases, adjacent subcells do not share common electrodes or charge transfer layers. Thus, a subcell may encompass the subunit construction regardless of whether each subunit has its own distinct electrodes or shares electrodes or charge transfer layers with adjacent subunits.

The open circuit voltage of the heterojunction cell is largely independent of the electrode materials and is determined by the value of HOMO-LUMO gap energy offset between the organic thin films, as well as their impurity doping concentrations. Therefore, one can expect that the performance of an ITO/organic bi-layer/metal cell, as well as metal/organic bi-layer/metal cell will be mostly affected by the parameters of the organic bi-layer materials. Subsequent deposition of two or more heterojunctions will lead to the formation of an inverse heterojunction between the acceptor layer of the front cell and the donor layer of the back cell. To prevent formation of this inverse heterojunction, an electron-hole recombination zone is inserted between the individual subcells. The electron-hole recombination zone provides a space for the recombination of electrons approaching from the front cell and holes from the back cell.

A PV device comprised of subcells electrically connected in series produces a higher voltage device. The donor-material and acceptor-material which provide the heterojunctions for the subcells may be the same for the various subcells or the donor- and acceptor materials may be different for the subcells of a particular device. It is important that each subcell in the device be

"balanced"; that is, that the amount of current generated by each subcell be about equal. It is preferred that each subcell generates the same current, with a deviation of less than about 10%. The current balancing is achieved by adjusting the thickness of the individual layers in a subcell and by choice of material which comprises the individual layers in a subcell. For example, if the incident radiation passes through in only one direction, the stacked subcells may have an increasing thickness with the outermost subcell, which is most directly exposed to the incident radiation, being the thinnest subcell. Alternatively, if the subcells are superposed on a reflective surface (for example, a metal cathode), the thicknesses of the individual subcells may be adjusted to account for the total combined radiation admitted to each subcell from the original and reflected directions. We have found that by balancing the subcells in a device, optimal performance can be achieved.

In addition to absorption, exciton diffusion length is an important considerations when choosing layer thickness. An exciton produced by an absorption must be sufficiently near to a donor-acceptor interface. The photo-generated exciton must diffuse to a donor-acceptor interface prior to geminate recombination to allow charge separation to occur. Both absorption and diffusion are easily modelled to achieve optimal cell thickness, as they are both exponential functions of distance.

The current generated by a device comprised of multiple subcells is equal to the smallest of the currents generated by the "series-connected" subcells. When the layers of the individual subcells are of a thickness much larger than the exciton diffusion length, L_d, the current is limited by the backmost subcell, since the current is proportional to the light intensity, which is attenuated by the forward subcells. To reduce the attenuation factor one can reduce the distance between front and back heterojunction interfaces, generally speaking, until the individual layer thickness becomes of the order of the active region width, i.e. of the order of L_d~30Å to ~100Å.

The organic photosensitive optoelectronic devices of the present invention may function as a solar cell, photodetector or photocell. Whenever the organic photosensitive optoelectronic devices of the present invention function as solar cells, the materials used in the photoconductive organic layers and the thicknesses thereof may be selected, for example, to optimize the external quantum

efficiency of the device. Whenever the organic photosensitive optoelectronic devices of the present invention function as photodetectors or photocells, the materials used in the photoconductive organic layers and the thicknesses thereof may be selected, for example, to maximize the sensitivity of the device to desired spectral regions.

In particular, the thicknesses of the individual layers may be adjusted so that in combination with selecting the total number of subcells in the stacked device, the external quantum efficiency of the device may be optimized so as to obtain an external quantum efficiency that is higher than that which is possible for a single cell. The term "external quantum efficiency" is used herein to refer to the efficiency with which a photosensitive optoelectronic device is capable of converting the total incident radiation into electrical power, as distinct from the term "internal quantum efficiency," which is used herein to refer to the efficiency with which a photosensitive optoelectronic device is capable of converting the absorbed radiation into electrical power. Using these terms, a stacked photosensitive optoelectronic device may be designed to achieve an external quantum efficiency, under a given set of ambient radiation conditions, that approaches the maximum internal quantum efficiency that may be achieved for an individual subcell under such ambient conditions.

This result may be achieved by considering several guidelines that may be used in the selection of layer thicknesses. It is desirable for the exciton diffusion length, L_D, to be greater than or comparable to the layer thickness, L, since it is believed that most exciton dissociation will occur at an interface. If L_D is less than L, then many excitons may recombine before dissociation. It is further desirable for the total photoconductive layer thickness to be of the order of the electromagnetic radiation absorption length, $1/\alpha$ (where α is the absorption coefficient), so that nearly all of the radiation incident on the solar cell is absorbed to produce excitons. Furthermore, the photoconductive layer thickness should be as thin as possible to avoid excess series resistance due to the high bulk resistivity of organic semiconductors.

Accordingly, these competing guidelines inherently require tradeoffs to be made in selecting the thickness of the photoconductive organic layers of a photosensitive optoelectronic cell. Thus, on the one hand, a thickness that is comparable or larger than the absorption length is desirable (for

a single cell device) in order to absorb the maximum amount of incident radiation. On the other hand, as the photoconductive layer thickness increases, two undesirable effects are increased. One is that due to the high series resistance of organic semiconductors, an increased organic layer thickness increases device resistance and reduces efficiency. Another undesirable effect is that increasing the photoconductive layer thickness increases the likelihood that excitons will be generated far from the effective field at a charge-separating interface, resulting in enhanced probability of geminate recombination and, again, reduced efficiency. Therefore, a device configuration is desirable which balances between these competing effects in a manner that produces a high quantum efficiency for the overall device. By using multiple stacked subcells, the photoconductive organic layers may be made very thin.

In particular, by taking the above-noted competing effects into account, that is, the absorption length of the photoconductive materials in the device, the diffusion length of the excitons in these materials, the photocurrent generation efficiency of these excitons, and the resistivity of these materials, the thickness of the layers in an individual cell may be adjusted so as to obtain a maximum internal quantum efficiency for those particular materials for a given set of ambient radiation conditions. Since the diffusion length of the excitons tends to have a relatively small value and the resistivity of typical photoconductive materials tends to be relatively large, an optimal subcell with respect to achieving the maximum internal quantum efficiency would typically be a relatively thin device. However, since the absorption length for such photoconductive organic materials tends to be relatively large as compared with the exciton diffusion length, such thin optimal photosensitive optoelectronic subcells, which may have the maximum internal quantum efficiency, would tend to have a relatively low external quantum efficiency, since only a small fraction of the incident radiation would be absorbed by such optimal subcells.

To improve the external quantum efficiency of an individual subcell, the thickness of the photoconductive organic layers may be increased so as to absorb significantly more incident radiation. Although the internal quantum efficiency for converting the additionally absorbed radiation into electrical power might gradually decrease as the thickness is increased beyond its optimal subcell thickness, the external quantum efficiency of the subcell would still increase until a

certain thickness is reached where no further increase in absorption could produce an increase in external quantum efficiency. Since the internal quantum efficiency of the subcell tends to drop rather sharply as the thickness of the photoconductive layers increases much beyond the diffusion length of the photo-generated excitons, the maximum external quantum efficiency of the subcell may be achieved well before the thickness of the thicker subcell is sufficient to absorb substantially all the incident radiation. Thus, the maximum external quantum efficiency that may be achieved using this single, thicker-cell approach is limited not only by the fact that the subcell thickness may be significantly greater than that desired for achieving the maximum internal quantum efficiency but, in addition, such thicker subcells may still not absorb all the incident radiation. Thus, due to both of these effects, the maximum external quantum efficiency of the thicker subcell would be expected to be significantly less than the maximum internal quantum efficiency that can be achieved for an optimal subcell having the optimal thickness.

When the thickness of an individual subcell is less than the active region thickness, further thinning of the subcell results in reduced absorption, which results in a linear decrease in efficiency. Since there is a balance of the currents in each subcell, the maximum number of subcells in a device of the invention corresponds to the cell thickness that still permits this balance. Each subcell in the stack should be as thick as the active region for that cell and still allow for cells deep within the stack to generate as much current as is consistent with the balance criterion.

Each subcell of a stacked device comprises an acceptor material and a donor material which provide a heterojunction. The donor material has an ionization potential that is smaller than that of the acceptor material. Further, the ionization potential HOMO/LUMO gap of the donor layer must be smaller than that of the acceptor layer. Generally, the materials comprising the donor or acceptor layers should have the longest possible exciton diffusion length, and thus are preferably those materials which lend themselves to ordered stacking of the molecules, such as planar, aromatic molecules.

The acceptor material may be comprised of, for example, perylenes, naphthalenes, fullerenes or nanotubules. A preferred acceptor material is 3,4,9,10-perylenetetracarboxylic bis-

benzimidazole (PTCBI).

Alternatively, the acceptor layer may be comprised of a fullerene material. The present invention provides devices incorporating an ETL comprising fullerenes, for example C_{60}, that show substantially improved power conversion efficiencies over previously demonstrated organic thin-film PV cells. It is believed that the improved results are primarily a consequence of the long exciton diffusion lengths of the fullerene, on the order of 77±10Å for C_{60} (L.A.A. Petterson et al., *J. Appl. Phys.* **86**, 487 (1999)). This can be compared to the exciton diffusion length of 30±3Å for PTCBI. In addition, electron conduction in the fullerene thin films does not lead to large voltage drops.

The fullerenes useful in this invention may have a broad range of sizes (number of carbon atoms per molecule). The term fullerene as used herein includes various cage-like molecules of pure carbon, including Buckminsterfullerene (C_{60}) and the related "spherical" fullerenes as well as carbon nanotubes. Fullerenes may be selected from those known in the art ranging from, for example, C_{20}-C_{1000}. Preferably, the fullerene is selected from the range of C_{60} to C_{96}. Most preferably the fullerene is C_{60} or C_{70}. It is also permissible to utilize chemically modified fullerenes, provided that the modified fullerene retains acceptor-type and electron mobility characteristics.

Adjacent to the acceptor layer, is a layer of organic donor-type material. The boundary of the acceptor layer and the donor layer forms the heterojunction which produces an internally generated electric field. A preferred material for the donor layer is a pthalocyanine or a porphyrin, or a derivative or transition metal complex thereof. Copper pthalocyanine (CuPc) is a particularly preferred donor material.

The individual subcells of the stacked devices may be separated by an electron-hole recombination zone. This layer serves to prevent the formation of an inverse heterojunction between the acceptor layer of the front cell and the donor layer of the back cell. The layer between the individual subcells provides a recombination zone for electrons approaching from the front subcell and holes from the back subcell. The effective recombination of electrons from the front subcell and holes from the back subcell is necessary if a photo-induced current is to be achieved in

the stacked device. Preferably, the electron-hole recombination zone comprises a thin metal layer. The metal layer must be thin enough to be semi-transparent in order to allow light to reach the back cell(s). To this end, it is preferred that the metal layer be less than about 20Å thick. It is especially preferred that the metal film be about 5 Å thick. It is believed that these ultra-thin metal films (~5Å) are not continuous films but rather are composed of isolated metal nanoparticles. Surprisingly, although the ultra-thin metal layer is not continuous, it still provides an efficient layer for electron-hole recombination. Preferred materials for use in this layer include Ag, Li, LiF, Al, Ti, and Sn. Silver is a particularly preferred metal for this layer. Gold is not believed to be a good choice for this layer as it is not known to introduce mid-gap states. In an alternative embodiment, the electron-hole recombination zone comprises a region of electronically active defects which lead to rapid electron-hole recombination. The defects may be introduced by limited damage at this interface, for example, by heating, by controlled impurity introduction, or by exposure to energetic particles during the deposition of the relevant organic layers. The energetic particles may be excited, for example, thermally or by an RF plasma.

The electrodes, or contacts, used in a photosensitive optoelectronic device are an important consideration, as shown in co-pending Applications Serial Nos. 09/136,342, both incorporated herein by reference. When used herein, the terms "electrode" and "contact" refer to layers that provide a medium for delivering photo-generated power to an external circuit or providing a bias voltage to the device. That is, an electrode, or contact, provides the interface between the photoconductively active regions of an organic photosensitive optoelectronic device and a wire, lead, trace or other means for transporting the charge carriers to or from the external circuit. In a photosensitive optoelectronic device, it is desirable to allow the maximum amount of ambient electromagnetic radiation from the device exterior to be admitted to the photoconductively active interior region. That is, the electromagnetic radiation must reach a photoconductive layer(s), where it can be converted to electricity by photoconductive absorption. This often dictates that at least one of the electrical contacts should be minimally absorbing and minimally reflecting of the incident electromagnetic radiation. That is, such a contact should be substantially transparent. The opposing electrode may be a reflective material so that light which has passed through the cell without being absorbed is reflected back through the cell. As used herein, a layer of material or a sequence of

several layers of different materials is said to be "transparent" when the layer or layers permit at least 50% of the ambient electromagnetic radiation in relevant wavelengths to be transmitted through the layer or layers. Similarly, layers which permit some, but less that 50% transmission of ambient electromagnetic radiation in relevant wavelengths are said to be "semi-transparent".

The electrodes are preferably composed of metals or "metal substitutes". Herein the term "metal" is used to embrace both materials composed of an elementally pure metal, e.g., Mg, and also metal alloys which are materials composed of two or more elementally pure metals, e.g., Mg and Ag together, denoted Mg:Ag. Here, the term "metal substitute" refers to a material that is not a metal within the normal definition, but which has the metal-like properties that are desired in certain appropriate applications. Commonly used metal substitutes for electrodes and charge transfer layers would include doped wide-bandgap semiconductors, for example, transparent conducting oxides such as indium tin oxide (ITO), gallium indium tin oxide (GITO), and zinc indium tin oxide (ZITO). In particular, ITO is a highly doped degenerate n+ semiconductor with an optical bandgap of approximately 3.2 eV, rendering it transparent to wavelengths greater than approximately 3900 Å. Another suitable metal substitute is the transparent conductive polymer polyanaline (PANI) and its chemical relatives. Metal substitutes may be further selected from a wide range of non-metallic materials, wherein the term "non-metallic" is meant to embrace a wide range of materials provided that the material is free of metal in its chemically uncombined form. When a metal is present in its chemically uncombined form, either alone or in combination with one or more other metals as an alloy, the metal may alternatively be referred to as being present in its metallic form or as being a "free metal". Thus, the metal substitute electrodes of the present invention may sometimes be referred to as "metal-free" wherein the term "metal-free" is expressly meant to embrace a material free of metal in its chemically uncombined form. Free metals typically have a form of metallic bonding that results from a sea of valence electrons which are free to move in an electronic conduction band throughout the metal lattice. While metal substitutes may contain metal constituents they are "non-metallic" on several bases. They are not pure free-metals nor are they alloys of free-metals. When metals are present in their metallic form, the electronic conduction band tends to provide, among other metallic properties, a high electrical conductivity as well as a high reflectivity for optical radiation.

Embodiments of the present invention may include, as one or more of the transparent electrodes of the photosensitive optoelectronic device, a highly transparent, non-metallic, low resistance cathode such as disclosed in U.S. Patent Application Serial No. 09/054,707 to Parthasarathy et al. ("Parthasarathy '707"), or a highly efficient, low resistance metallic/non-metallic compound cathode such as disclosed in U.S. Patent No. 5,703,436 to Forrest et al. ("Forrest '436"), both incorporated herein by reference. Each type of cathode is preferably prepared in a fabrication process that includes the step of sputter depositing an ITO layer onto either an organic material, such as copper phthalocyanine (CuPc), to form a highly transparent, non-metallic, low resistance cathode or onto a thin Mg:Ag layer to form a highly efficient, low resistance metallic/non-metallic compound cathode. Parthasarathy '707 discloses that an ITO layer onto which an organic layer had been deposited, instead of an organic layer onto which the ITO layer had been deposited, does not function as an efficient cathode.

Herein, the term "cathode" is used in the following manner. In a non-stacked PV device or a single unit of a stacked PV device under ambient irradiation and connected with a resistive load and with no externally applied voltage, e.g., a solar cell, electrons move to the cathode from the adjacent photo-conducting material. Similarly, the term "anode" is used herein such that in a solar cell under illumination, holes move to the anode from the adjacent photo-conducting material, which is equivalent to electrons moving in the opposite manner. It will be noted that as the terms are used herein, anodes and cathodes may be electrodes or charge transfer layers.

In a preferred embodiment of the invention, the stacked organic layers include one or more exciton blocking layers (EBLs) as described in U.S. Patent No. 6,097,147, Peumans et al, *Applied Physics Letters* **2000**, *76*, 2650-52, and co-pending application serial number 09/449,801, filed Nov. 26, 1999, both incorporated herein by reference. Higher internal and external quantum efficiencies have been achieved by the inclusion of an EBL to confine photogenerated excitons to the region near the dissociating interface and to prevent parasitic exciton quenching at a photosensitive organic/electrode interface. In addition to limiting the volume over which excitons may diffuse, an EBL can also act as a diffusion barrier to substances introduced during deposition of the electrodes. In some circumstances, an EBL can be made thick enough to fill pinholes or

shorting defects which could otherwise render an organic PV device non-functional. An EBL can therefore help protect fragile organic layers from damage produced when electrodes are deposited onto the organic materials.

It is believed that the EBLs derive their exciton blocking property from having a LUMO-HOMO energy gap substantially larger than that of the adjacent organic semiconductor from which excitons are being blocked. Thus, the confined excitons are prohibited from existing in the EBL due to energy considerations. While it is desirable for the EBL to block excitons, it is not desirable for the EBL to block all charge. However, due to the nature of the adjacent energy levels, an EBL will necessarily block one sign of charge carrier. By design, an EBL will always exist between two layers, usually an organic photosensitive semiconductor layer and a electrode or charge transfer layer. The adjacent electrode or charge transfer layer will be in context either a cathode or an anode. Therefore, the material for an EBL in a given position in a device will be chosen so that the desired sign of carrier will not be impeded in its transport to the electrode or charge transfer layer. Proper energy level alignment ensures that no barrier to charge transport exists, preventing an increase in series resistance. For example, it is desirable for a material used as a cathode side EBL to have a LUMO level closely matching the LUMO level of the adjacent ETL material so that any undesired barrier to electrons is minimized.

It should be appreciated that the exciton blocking nature of a material is not an intrinsic property of its HOMO-LUMO energy gap. Whether a given material will act as an exciton blocker depends upon the relative HOMO and LUMO levels of the adjacent organic photosensitive material. Therefore, it is not possible to identify a class of compounds in isolation as exciton blockers without regard to the device context in which they may be used. However, with the teachings herein one of ordinary skill in the art may identify whether a given material will function as an exciton blocking layer when used with a selected set of materials to construct an organic PV device.

In a preferred embodiment of the invention, an EBL is situated between the acceptor layer and the cathode (back subcell). A preferred material for the EBL comprises 2,9-dimethyl-4,7-

diphenyl-1,10-phenanthroline (also called bathocuproine or BCP), which is believed to have a LUMO-HOMO separation of about 3.5 eV, or bis(2-methyl-8-hydroxyquinolinoato)-aluminum(III)phenolate (Alq_2OPH). BCP is an effective exciton blocker which can easily transport electrons to the cathode from the adjoining acceptor layer. Generally, an EBL will not be included in the forward subcells. Positioning an EBL adjacent to the electron-hole recombination zone may prevent the charge carriers from reaching the recombination zone and thereby reduce cell efficiency.

The EBL layer may be doped with a suitable dopant, including but not limited to 3,4,9,10-perylenetracarboxylic dianhydride (PTCDA), 3,4,9,10-perylenetracarboxylic diimide (PTCDI), 3,4,9,10-perylenetetracarboxylic-bis-benzimidazole (PTCBI), 1,4,5,8-naphthalenetetracarboxylic dianhydride (NTCDA), and derivatives thereof. It is thought that the BCP as deposited in the present devices is amorphous. The present apparently amorphous BCP exciton blocking layers may exhibit film recrystallization, which is especially rapid under high light intensities. The resulting morphology change to polycrystalline material results in a lower quality film with possible defects such as shorts, voids or intrusion of electrode material. Accordingly, it has been found that doping of some EBL materials, such as BCP, that exhibit this effect with a suitable, relatively large and stable molecule can stabilize the EBL structure to prevent performance degrading morphology changes. It should be further appreciated that doping of an EBL which is transporting electrons in a giving device with a material having a LUMO energy level close to that of the EBL will help insure that electron traps are not formed which might produce space charge build-up and reduce performance. Additionally, it should be appreciated that relatively low doping densities should minimize exciton generation at isolated dopant sites. Since such excitons are effectively prohibited from diffusing by the surrounding EBL material, such absorptions reduce device photoconversion efficiency.

Representative embodiments may also comprise transparent charge transfer layers. As described herein charge transfer layers are distinguished from ETL and HTL layers by the fact that charge transfer layers are frequently, but not necessarily, inorganic and they are generally chosen not to be photoconductively active. The term "charge transfer layer" is used herein to refer to layers similar to but different from electrodes in that a charge transfer layer only delivers charge carriers

from one subsection of an optoelectronic device to the adjacent subsection.

In another preferred embodiment of the invention, a charge transfer layer is situated between the anode and the donor layer. A preferred material for this layer comprises a film of 3,4-polyethylenedioxythiophene:polystyrenesulfonate (PEDOT:PSS). The PEDOT:PSS layer functions as an anode smoothing layer. The introduction of the PEDOT:PSS layer between the anode (ITO) and the donor layer (CuPc) leads to fabrication yields of close to 100%. We attribute this to the ability of the spin-coated PEDOT:PSS film to planarize the ITO, whose rough surface could otherwise result in shorts through the thin molecular film.

In a further embodiment on the invention, one or more of the layers may be treated with plasma prior to depositing the next layer. The layers may be treated, for example, with a mild argon or oxygen plasma. This treatment is beneficial as it reduces the series resistance. It is particularly advantageous that the PEDOT:PSS layer be subject to a mild plasma treatment prior to deposition of the next layer.

A concentrator configuration can be employed to increase the efficiency of the device, where photons are forced to make multiple passes through the thin absorbing regions. Co-pending U.S. Patent Application No. 09/449,800 entitled "*Highly Efficient Multiple Reflection Photosensitive Optoelectronic Device with Optical Concentrator*" (hereinafter " '800 Application"), incorporated herein by reference, addresses this issue by using structural designs that enhance the photoconversion efficiency of photosensitive optoelectonic devices by optimizing the optical geometry for high absorption and for use with optical concentrators that increase collection efficiency. Such geometries for photosensitive devices substantially increase the optical path through the material by trapping the incident radiation within a reflective cavity or waveguiding structure, and thereby recycling light by multiple reflection through the thin film of photoconductive material. The geometries disclosed in the '800 Application therefore enhance the external quantum efficiency of the devices without causing substantial increase in bulk resistance. Included in the geometry of such devices is a first reflective layer; a transparent insulating layer which should be longer than the optical coherence length of the incident light in all dimensions to prevent optical

microcavity interference effects; a transparent first electrode layer adjacent the transparent insulating layer; a photosensitive heterostructure adjacent the transparent electrode; and a second electrode which is also reflective.

The '800 Application also discloses an aperture in either one of the reflecting surfaces or an external side face of the waveguiding device for coupling to an optical concentrator, such as a Winston collector, to increase the amount of electromagnetic radiation efficiently collected and delivered to the cavity containing the photoconductive material. Exemplary non-imaging concentrators include a conical concentrator, such as a truncated paraboloid, and a trough-shaped concentrator. With respect to the conical shape, the device collects radiation entering the circular entrance opening of diameter d_1 within $\pm \theta_{max}$ (the half angle of acceptance) and directs the radiation to the smaller exit opening of diameter d_2 with negligible losses and can approach the so-called thermodynamic limit. This limit is the maximum permissible concentration for a given angular field of view. Conical concentrators provide higher concentration ratios than trough-shaped concentrators but require diurnal solar tracking due to the smaller acceptance angle. (After *High Collection Nonimaging Optics* by W.T. Welford and R. Winston, (hereinafter "Welford and Winston") pp 172-175, Academic Press, 1989, incorporated herein by reference).

Devices have been constructed and example data recorded for exemplary embodiments of the present invention. The following examples of the invention are illustrative and not limiting of the invention.

EXAMPLES

Example 1

Exemplary embodiments are fabricated on pre-cleaned ITO glass substrates, spin-coated with a 300 Å thick layer of polyethylenedioxythiophene: poystyrenesulfonate (PEDOT). Spin coating is performed at 4000 rpm for 40 sec, and is followed by 30 min drying at 110°C for 1 hour at reduced pressure. The organic materials are purified by train sublimation. The PV cells are formed by thermal evaporation (room temperature, 10^{-6} Torr, deposition rate of 1.5-2 Å/sec) of organic materials on the ITO/PEDOT glass in the following sequence: donor-acceptor-metal-

donor-acceptor-metal. The thickness of individual layers is controlled by use of, for example, a crystal oscillator thickness monitor. Copper phthalocyanine, CuPc, is used as a donor, and perylenetetracarboxylic bis-benzimidazole (PTCBI) as an acceptor. Ag is used for the thin (~ 5-20 Å) layer between the front and the back cells and as a top metal electrode material. The top electrode (of 800 Å thickness) is deposited through shadow mask of circular shape of 1 mm diameter.

Power conversion efficiency was measured in air under illumination of a solar simulator giving AM1.5 white light. The light intensity was varied using neutral density filters. The current-voltage (I-V) characteristics of single (closed squares) and tandem (open squares) cells at 1 sun incident light intensity are shown in Figure 1. The cell structure is as follows: substrate/300Å CuPc/300Å PTCBI/20Å Ag/300Å CuPc/300Å PTCBI/800Å Ag - for tandem, and substrate/300Å CuPc/300Å PTCBI/800Å Ag for regular, single cell. The open circuit voltage produced by the tandem cell is doubled, as compared to the single cell. Although the photovoltage from the tandem cell is doubled, the short circuit current of the tandem cell is significantly lower than that of the single cell.

We have compared clean ITO glass with ITO covered with PEDOT as a substrate for PV devices. It turns out that for the thinnest devices (with individual layer thickness of less than about 100 Å), a pre-deposited PEDOT layer prevents appearance of short circuits, presumably due to lower surface roughness, as compared to ITO. Indeed, the AFM measurements revealed the roughness values of about 20 Å and 45 Å for PEDOT and bare ITO respectively.

For devices with layer thickness less than 300 Å, the V_{oc} is somewhat higher for devices prepared on PEDOT-substrate, while the short circuit current (I_{so}) is slightly lower. Increased photovoltage produced by devices containing PEDOT layer is especially pronounced in CuPc/C_{60} device, indicating that the photovoltage may be originated in both energy bands mismatch and the difference of the electrodes work functions.

In contrast to thinner films, for the devices having layer thickness of about 350 Å and

thicker, use of bare ITO substrate is advantageous. This is due to the fact that the morphology of the substrate become less important for such devices, while additional layer of PEDOT is a source of parasitic absorption as well as additional series resistance.

Further improvement can be done with the help of exciton blocking layer (EBL) concept. Incorporating large band gap, electron conducting layer (such as BCP) between the acceptor (PTCBI) and electron collecting electrode leads to increase of external quantum efficiency. This was related to BCP ability to prevent exciton diffusion and subsequent exciton quenching at the electrode. In order to check this concept for tandem devices we have prepared PV cells with and without BCP layer. Figure 5 shows I-V characteristics for tandem devices with (filled squares) and without (open squares) 100 Å BCP layer incorporated in the back cell. The characteristics were measured under 1 sun illumination. Significant increase of the photocurrent density can be clearly seen, thus confirming usefulness of the EBL concept application to tandem PV cells.

While including BCP layer as a part of the back cell (i.e. before thick Ag electrode) seems to be advantageous, introducing it as a part of the front cell (i.e. before thin Ag interlayer) leads to sharp decrease in the device performance. This indicates that transport sites in BCP appear as a secondary result of the deposition of thick Ag layer.

Example 2

Exemplary embodiments are fabricated on pre-cleaned glass substrates coated with a ~1400Å thick transparent, conducting indium-tin-oxide (ITO) anode (with a sheet resistance of 40 Ω/sq.). After solvent cleaning, the substrates are treated with an O_2-plasma (50W, 100mTorr, 5 minutes). Unless otherwise specified, the ITO film is then coated with a (320±10)Å thick film of PEDOT:PSS by spin coating from solution at 4000rpm for 40 seconds, followed by drying at 90°C for 15 minutes in vacuum. The organic materials can be obtained commercially, and then purified using thermal gradient sublimation. Films are grown at room temperature in high vacuum (~1 x 10^{-6} Torr) in the following sequence: a 50Å to 400Å thick film of the donor-like copper phthalocyanine (CuPc), followed by a 100Å to 400Å thick film of the acceptor-like C_{60}. Next, a 50Å to 400Å thick bathocuproine (BCP) EBL is deposited. The cathode consists of Al, deposited by thermal

evaporation through a shadow mask with 1mm diameter circular openings. Power conversion efficiencies are measured under illumination from a solar simulator set to produce an AM1.5G (air mass 1.5, global) spectrum. The intensity is measured using a calibrated broadband optical power meter and is varied using neutral density filters. Quantum efficiencies are measured at ~400Hz using monochromatic light of variable wavelength with a 50% duty cycle.

In Figure 11 we compare the current-voltage (I-V, upper panel) and photocurrent-voltage (lower panel) characteristics in the dark (open symbols) and under solar illumination (filled symbols) of two cells with the structure anode/200Å CuPc/200Å C_{60}/150Å BCP/800Å Al grown simultaneously on different substrates. Cell A (squares) was grown on bare ITO, while for cell B (circles), the ITO was precoated with PEDOT:PSS. The introduction of the PEDOT:PSS layer leads to an increase in the dark current (open circles) under forward bias by a factor of ~10. In contrast, the reverse-biased dark current remains unchanged. Furthermore, the presence of the PEDOT:PSS also causes a shift of the photocurrent characteristics by a voltage $\Delta V=(0.50\pm0.05)V$, in agreement with recent electroabsorption studies on polymer light-emitting diodes with and without a PEDOT:PSS hole injection layer T.M. Brown et al., *Appl. Phys. Lett.* **75**, 1679 (1999). These changes are explained by the higher work function of the PEDOT:PSS in comparison with that of ITO, moving the Fermi-level 0.50V closer to the CuPc highest occupied molecular orbital (HOMO). This results in improved current injection into the CuPc layer because of the smaller barrier to hole injection and hence an increased dark current under forward bias. This also increases the charge-separating built-in electrostatic potential (V_{bi}) by 0.50V (Figure 10), leading to improved collection of the photogenerated carriers at higher positive voltages, and hence an increased power conversion efficiency.

Figure 12 shows the effect of mild plasma treatment (10W, 30s, 100mTorr, 100sccm Ar or O_2) of the PEDOT:PSS layer on the I-V characteristics of devices with the layer structure ITO/PEDOT:PSS/50Å CuPc/200Å C_{60}/100Å BCP/800Å Al under AM1.5G solar illumination with an intensity of 400mW/cm^2 (4 suns). The fill-factor (*ff*) increases from 0.36 for untreated PEDOT:PSS, to 0.41 for O_2, and 0.49 for Ar treated PEDOT:PSS films. The treatment apparently modifies the surface electronic structure of the PEDOT:PSS layer, leading to improved

carrier collection properties. We also note that the introduction of PEDOT:PSS in our PV cells leads to a fabrication yield close to 100% (i.e. no shorts were observed for >50 measured devices of varying thicknesses). We attribute this to the ability of the spin-coated PEDOT:PSS film to planarize the ITO, whose rough surface would otherwise result in shorts through the thin molecular film.

The C_{60} lowest unoccupied molecular orbital (LUMO) energy as estimated from the difference of the ionization potential and the optical energy gap, lies below that of BCP by (1.0±0.2)eV (Figure 10). Despite the fact that the optical energy gap leads to only an indirect estimate of the position of the LUMO levels, the photogenerated electrons must nevertheless be transported from the C_{60} LUMO, over the barrier formed by the BCP LUMO, into the cathode without incurring a substantial voltage drop or cell series resistance. This suggests that electron transport across the BCP mainly occurs through states below the LUMO induced during deposition of the metal cathode. Evidence for this is given in the inset of Fig. 11, which shows the short circuit current density (J_{SC}) of ITO/PEDOT:PSS/200Å CuPc/400Å C_{60}/BCP/Al devices as a function of the thickness of the BCP layer under AM1.5G illumination with an intensity of 100mW/cm^2. The initial increase in J_{SC} is due to an increase in absorption efficiency as the active layers are separated from the metallic cathode. J_{SC} then rolls off exponentially with BCP thicknesses >150Å. This suggests that defect states below the LUMO of BCP, induced by the thermalization of the hot metal atoms promote electron transport from the C_{60} layer to the cathode. These states are generated over a distance of ~150Å into the BCP with a density sufficient to extract carriers at a rate exceeding that of photocarrier generation.

In Figure 13, we show the I-V characteristics of the optimized device structure: ITO/PEDOT:PSS(Ar treated)/200Å CuPc/400Å C_{60}/120Å BCP/1000Å Al, as a function of the incident optical power density. The external power conversion efficiency (η_P), open circuit voltage (V_{OC}) and FF of this device as functions of the incident optical power density are plotted in Fig. 14a. The conversion efficiency, η_P, reaches a maximum of (3.7±0.2)% at an incident power level of 44mW/cm^2 (0.44 suns) and rolls off at higher illumination intensities because of the cell series resistance (R_S) of (6.2±1.2)Ω-cm^2. At an illumination intensity of 150mW/cm^2, η_P=(3.6±0.2)%,

J_{SC}=18.8mA/cm^2, V_{OC}=0.58V, and *ff*=0.52, while at 1200mW/cm^2 illumination, J_{SC} reaches a value as high as 138mA/cm^2. The effect of the series resistance can be clearly seen in Figure 13. At intensities >150mW/cm^2, the maximum electrical output power is achieved at lower voltages, leading to lower values for *ff*, and hence η_P. In contrast to results for CuPc/PTCBI/BCP cells, no broad plateau of maximum power conversion efficiency is observed as a consequence of the higher power conversion efficiency which magnifies the effect of the series resistance. In Figure 14b, the external quantum efficiency of this device and the solar spectral density are plotted as functions of wavelength. The photocurrent contribution of C_{60} is generated between λ=400nm and 550nm, while the CuPc layer contributes from λ=550nm to 750nm, such that the solar spectrum at λ<750nm is completely covered.

In summary, we have shown that the efficiency of organic solar cells employing an EBL can be significantly higher than conventional cells, depending on materials choice and processing parameters. In particular, the use of C_{60} with its long exciton diffusion length, together with optimization of the contacts leads to external power conversion efficiencies of (3.6±0.2)% under AM1.5G solar illumination with an intensity of 150mW/cm^2. We anticipate that additional improvements to these devices, such as the use of light trapping structures with these CuPc/C_{60} double heterostructure cells will lead to power conversion efficiencies in excess of 5%. Thus, the present invention is directed to organic solar cells having an external power conversion efficiency of at least about 3.6%.

Although the present invention is described with respect to particular examples and preferred embodiments, it is understood that the present invention is not limited to these examples and embodiments. The present invention as claimed may therefore include variations from the particular examples and preferred embodiments described herein, as will be apparent to one of skill in the art.

CLAIMS

What is claimed is:

1. An organic photosensitive optoelectronic device comprising:

an anode;

multiple subcells in series, each subcell comprising:

an electron donor layer, and

an electron acceptor layer in contact with the electron donor layer,

an electron-hole recombination zone separating the subcells, and

a cathode,

wherein the current generated by each subcell is about equal.

2. The device of claim 1, wherein an exciton blocking layer is situated between the electron acceptor layer and the cathode.

3. The device of claim 2, wherein the exciton blocking layer comprises BCP.

4. The device of claim 2, wherein the exciton blocking layer comprises Alq_2OPH.

5. The device of claim 1, wherein the anode smoothing layer is situated between the electron donor layer and the anode.

6. The device of claim 1, wherein the anode smoothing layer comprises PEDOT:PSS.

7. The device of claim 1, wherein the electron donor layer comprises a pthalocyanine or a porphyrin, and the electron acceptor layer comprises a perylene, naphthalene, fullerene or nanotubule.

8. The device of claim 1, wherein the anode is selected from transparent conducting oxides.

9. The device of claim 8, wherein the anode is selected from ITO.

10. The device of claim 1, wherein the electron-hole recombination zone is a semitransparent metal layer.

11. The device of claim 1, wherein the electron-hole recombination zone is selected from a layer of Ag, Li, LiF, Al, Ti, and Sn.

12. The device of claim 11, wherein the electron-hole recombination zone a layer of Ag.

13. The device of claim 1, wherein the electron-hole recombination zone is less than about 20 Å

14. The device of claim 10, wherein the metal layer is composed of nanoparticles.

15. The device of claim 1, wherein the electron-hole recombination zone comprises a region of electronically active defects.

16. The device of claim 2, wherein:

the electron transport layer is PTCBI

the hole transport layer is CuPc;

the electron-hole recombination zone is Ag, and

the exciton blocking layer is BCP.

17. The device of claim 2, wherein:

the electron transport layer a fullerene

the hole transport layer is CuPc;

the electron-hole recombination zone is Ag, and

the exciton blocking layer is BCP.

18. The device of claim 1, wherein the external power conversion efficiency is at least 1% at one sun illumination.

19. An organic photosensitive optoelectronic device comprising:

an anode;

a hole transport layer, the hole transport layer formed of a photoconductive organic semiconductor material;

an electron transport layer over the hole transport layer, the electron transport layer comprising a fullerene;

an exciton blocking layer; and

a cathode.

20. The device of claim 19, wherein the exciton blocking layer is situated between the electron transport layer and the cathode.

21. The device of claim 20, wherein the exciton blocking layer comprises BCP.

22. The device of claim 20, wherein the exciton blocking layer comprises Alq_2OPH.

23. The device of claim 19, wherein an anode smoothing layer is situated between the electron donor layer and the anode..

24. The device of claim 23, wherein the anode smoothing layer comprises PEDOT:PSS.

25. The device of claim 24, wherein the PEDOT:PSS has been treated with plasma.

26. The device of claim 19, wherein the fullerene is selected from the size range of C_{60} to C_{96}.

27. The device of claim 19, wherein the fullerene is a nanotube.

28. The device of claim 19, wherein the anode is selected from transparent conducting oxides.

29. The device of claim 28, wherein the anode is selected from ITO.

30. The device of claim 20, wherein:

the electron transport layer is C_{60},

the hole transport layer is CuPc; and

the exciton blocking layer is BCP.

31. The device of claim 19, wherein the external power conversion efficiency is at least about 3.6%.

32. The device of claim 19, wherein the electron transport layer, the hole transport layer, and the exciton blocking layer are disposed between two parallel planar reflective surfaces which form a waveguide.

33. The device of claim 32, wherein one of the two reflective surfaces has an aperture to admit light incident upon the device.

34. The device of claim 33, having a transparent opening between the two reflective surfaces so that light is admitted to the device from a direction parallel to the planes of the reflective surfaces.

35. A stacked organic photosensitive optoelectronic device comprised of a plurality of photosensitive optoelectronic subcells, wherein at least one subcell includes an electron transporting layer comprising a fullerene.

36. The device of claim 35, wherein the subcell additionally includes an exciton blocking layer and a hole transport layer adjacent the electron transport layer.

37. The device of claim 36, wherein the exciton blocking layer comprises BCP and is adjacent the electron transport layer.

38. The device of claim 35, wherein:

the electron transport layer is C_{60},

the hole transport layer is CuPc; and

the exciton blocking layer is BCP

39. A method for making an organic photosensitive optoelectronic device, the device comprising an anode, a hole transport layer, an electron transport layer comprising a fullerene, an exciton blocking layer and a cathode, the method comprising the steps of:

(a) depositing the hole transport layer over the anode;

(b) depositing the electron transport layer over the hole transport layer,

(c) depositing the exciton blocking layer over the electron transport layer ; and

(d) depositing the cathode over the exciton blocking layer.

Figure 1.

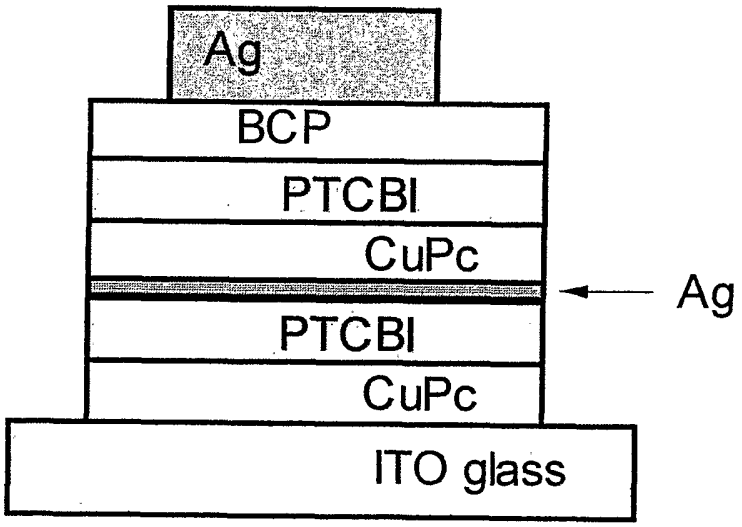

Figure 2

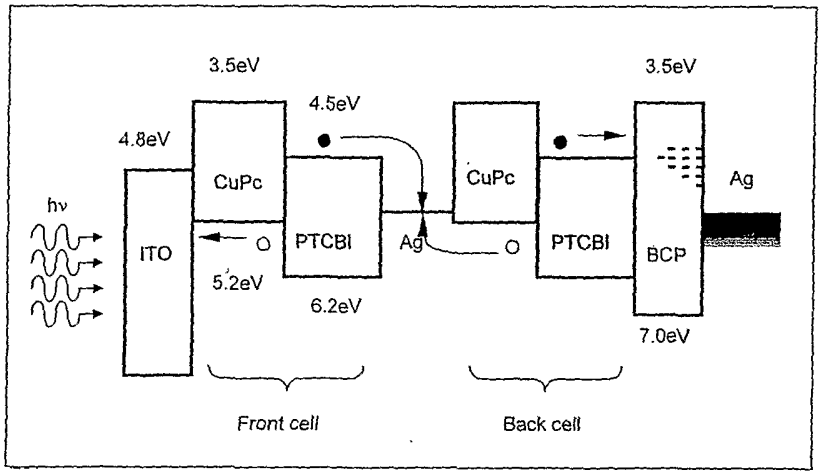
3.5eV
4.5eV
3.5eV
4.8eV
CuPc
CuPc
Ag
hν
ITO
O
PTCBI
Ag
O
PTCBI
BCP
5.2eV
6.2eV
7.0eV
Front cell
Back cell

Figure 3

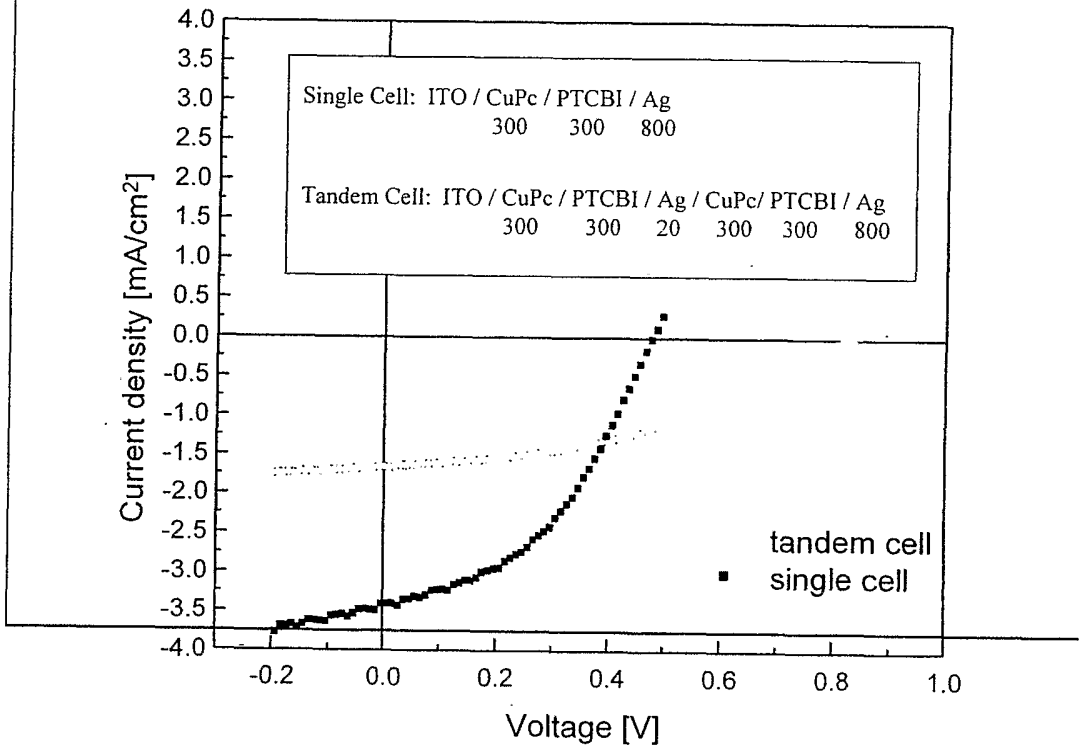
Single Cell: ITO / CuPc / PTCBI / Ag
300 300 800
Tandem Cell: ITO / CuPc / PTCBI / Ag / CuPc/ PTCBI / Ag
300 300 20 300 300 800
tandem cell
single cell
Current density [mA/cm²]
Voltage [V]
4.0
3.5
3.0
2.5
2.0
1.5
1.0
0.5
0.0
-0.5
-1.0
-1.5
-2.0
-2.5
-3.0
-3.5
-4.0
-0.2
0.0
0.2
0.4
0.6
0.8
1.0

Figure 4

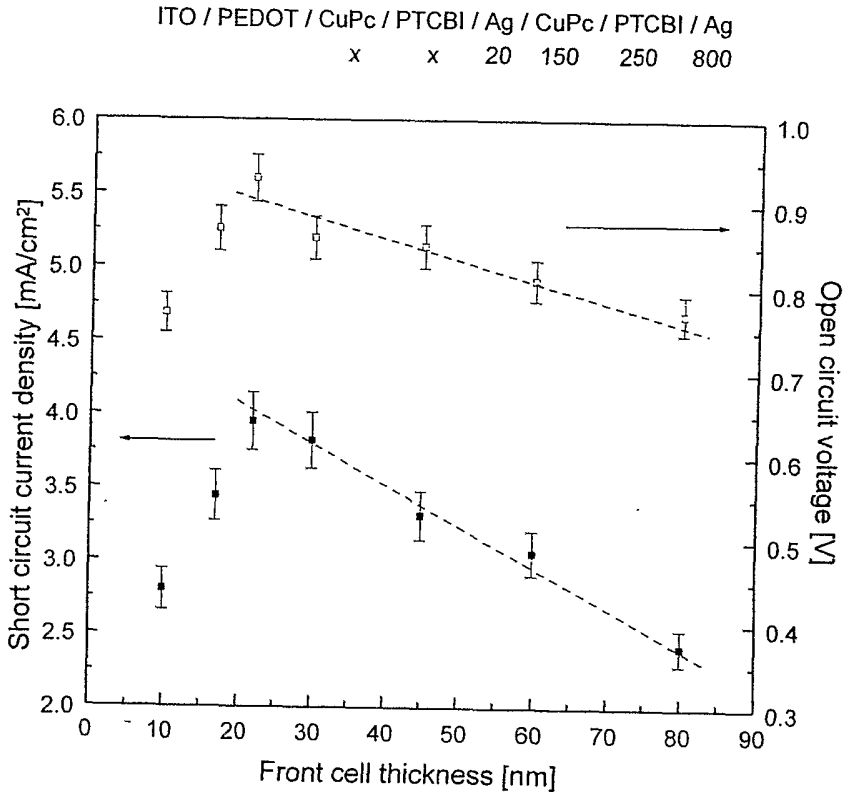
ITO / PEDOT / CuPc / PTCBI / Ag / CuPc / PTCBI / Ag
x x 20 150 250 800
Short circuit current density [mA/cm²]
Open circuit voltage [V]
Front cell thickness [nm]
6.0
5.5
5.0
4.5
4.0
3.5
3.0
2.5
2.0
1.0
0.9
0.8
0.7
0.6
0.5
0.4
0.3
0
10
20
30
40
50
60
70
80
90

Figure 5

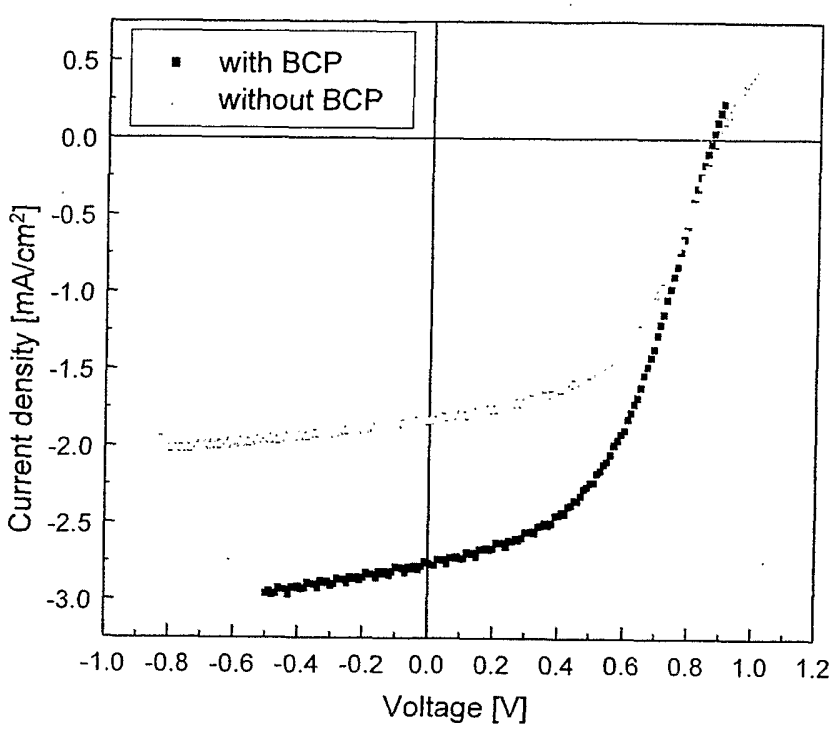
with BCP
without BCP
Current density [mA/cm²]
0.5
0.0
-0.5
-1.0
-1.5
-2.0
-2.5
-3.0
-1.0 -0.8 -0.6 -0.4 -0.2 0.0 0.2 0.4 0.6 0.8 1.0 1.2
Voltage [V]

Figure 6

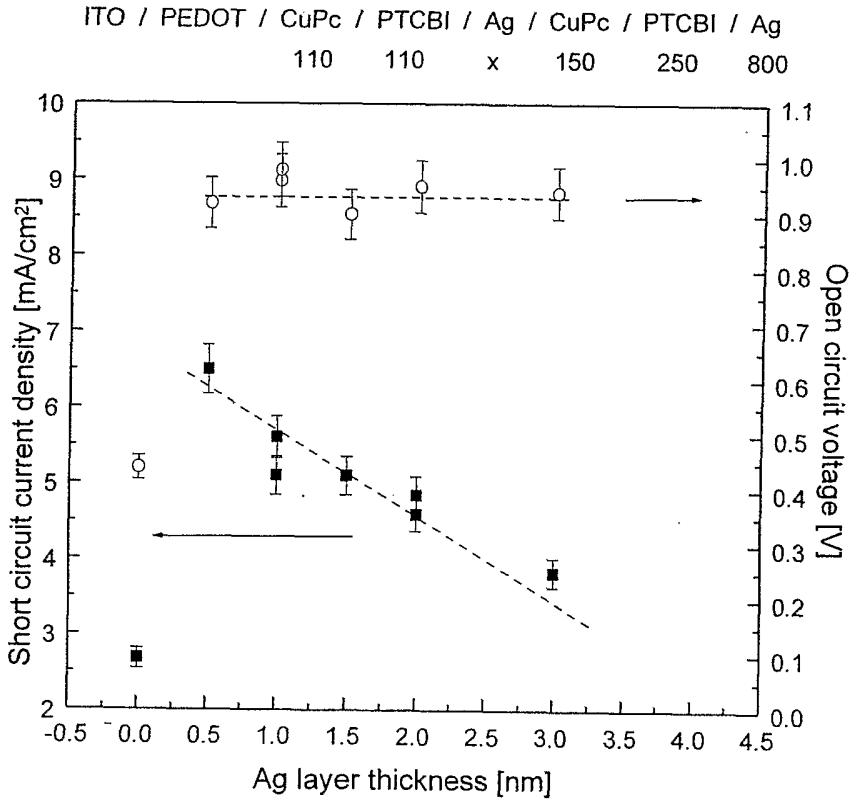
ITO / PEDOT / CuPc / PTCBI / Ag / CuPc / PTCBI / Ag
110 110 x 150 250 800
Short circuit current density [mA/cm²]
Open circuit voltage [V]
Ag layer thickness [nm]
10
9
8
7
6
5
4
3
2
1.1
1.0
0.9
0.8
0.7
0.6
0.5
0.4
0.3
0.2
0.1
0.0
-0.5
0.0
0.5
1.0
1.5
2.0
2.5
3.0
3.5
4.0
4.5

Figure 7

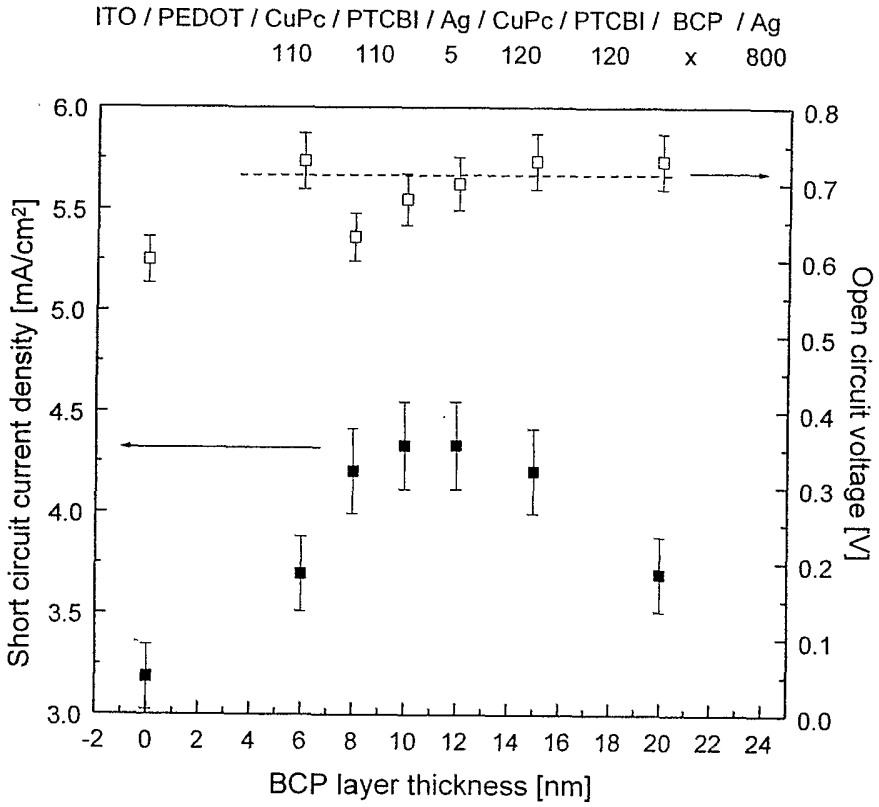
ITO / PEDOT / CuPc / PTCBI / Ag / CuPc / PTCBI / BCP / Ag
110 110 5 120 120 x 800
Short circuit current density [mA/cm²]
Open circuit voltage [V]
BCP layer thickness [nm]
6.0
5.5
5.0
4.5
4.0
3.5
3.0
0.8
0.7
0.6
0.5
0.4
0.3
0.2
0.1
0.0
-2 0 2 4 6 8 10 12 14 16 18 20 22 24

Figure 8

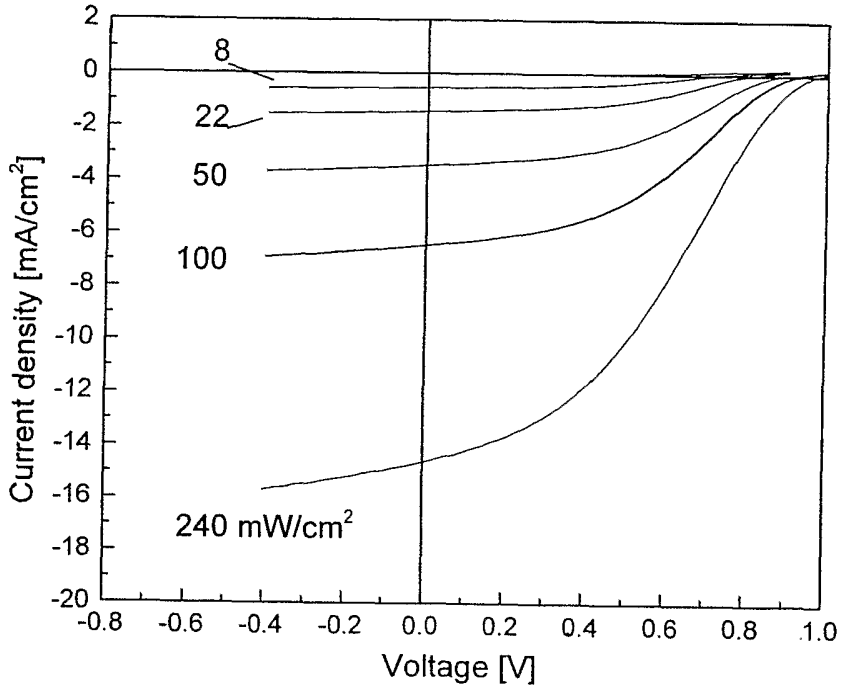
Current density [mA/cm^2]
Voltage [V]
8
22
50
100
240 mW/cm^2
2
0
-2
-4
-6
-8
-10
-12
-14
-16
-18
-20
-0.8
-0.6
-0.4
-0.2
0.0
0.2
0.4
0.6
0.8
1.0

Figure 9

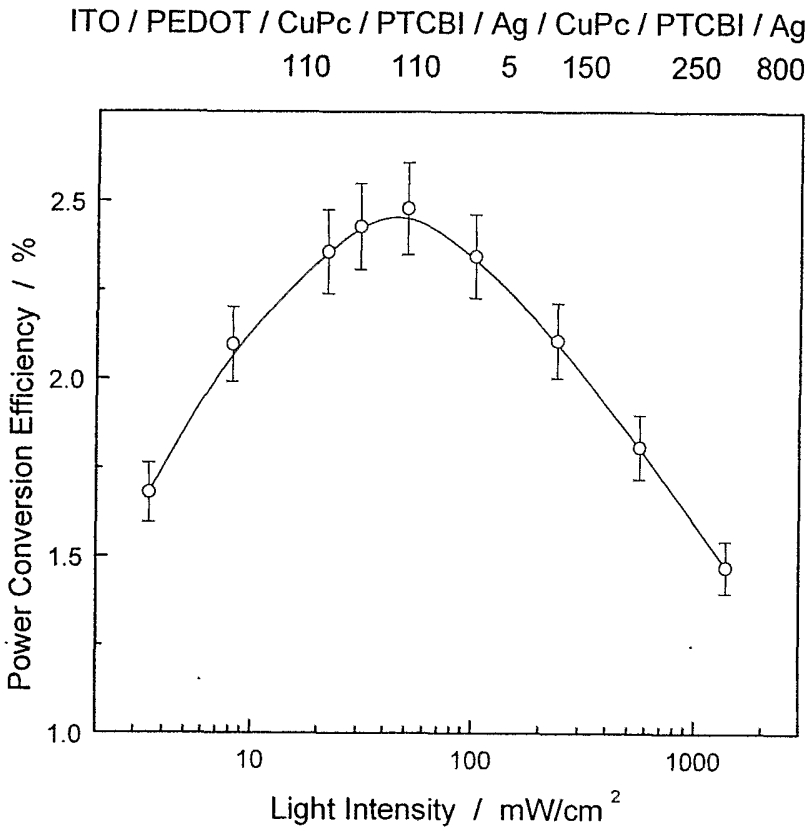
ITO / PEDOT / CuPc / PTCBI / Ag / CuPc / PTCBI / Ag
110 110 5 150 250 800
Power Conversion Efficiency / %
2.5
2.0
1.5
1.0
10
100
1000
Light Intensity / mW/cm 2

Figure 10

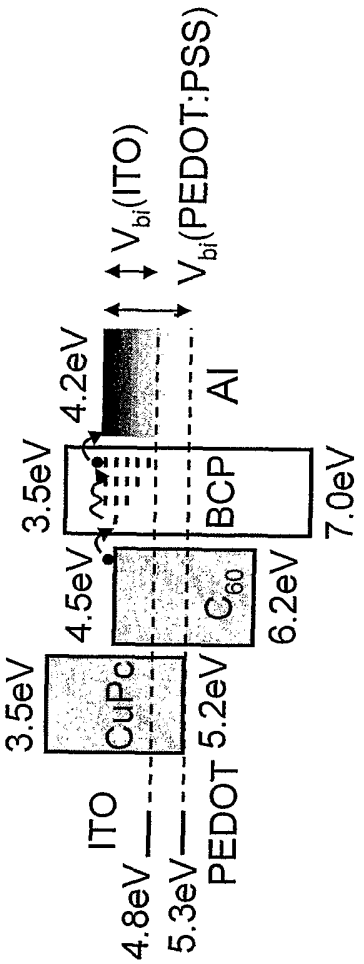
ITO
4.8eV
PEDOT
5.3eV
3.5eV
CuPc
5.2eV
4.5eV
C_{60}
6.2eV
3.5eV
BCP
7.0eV
4.2eV
Al
V_{bi}(ITO)
V_{bi}(PEDOT:PSS)

Figure 11

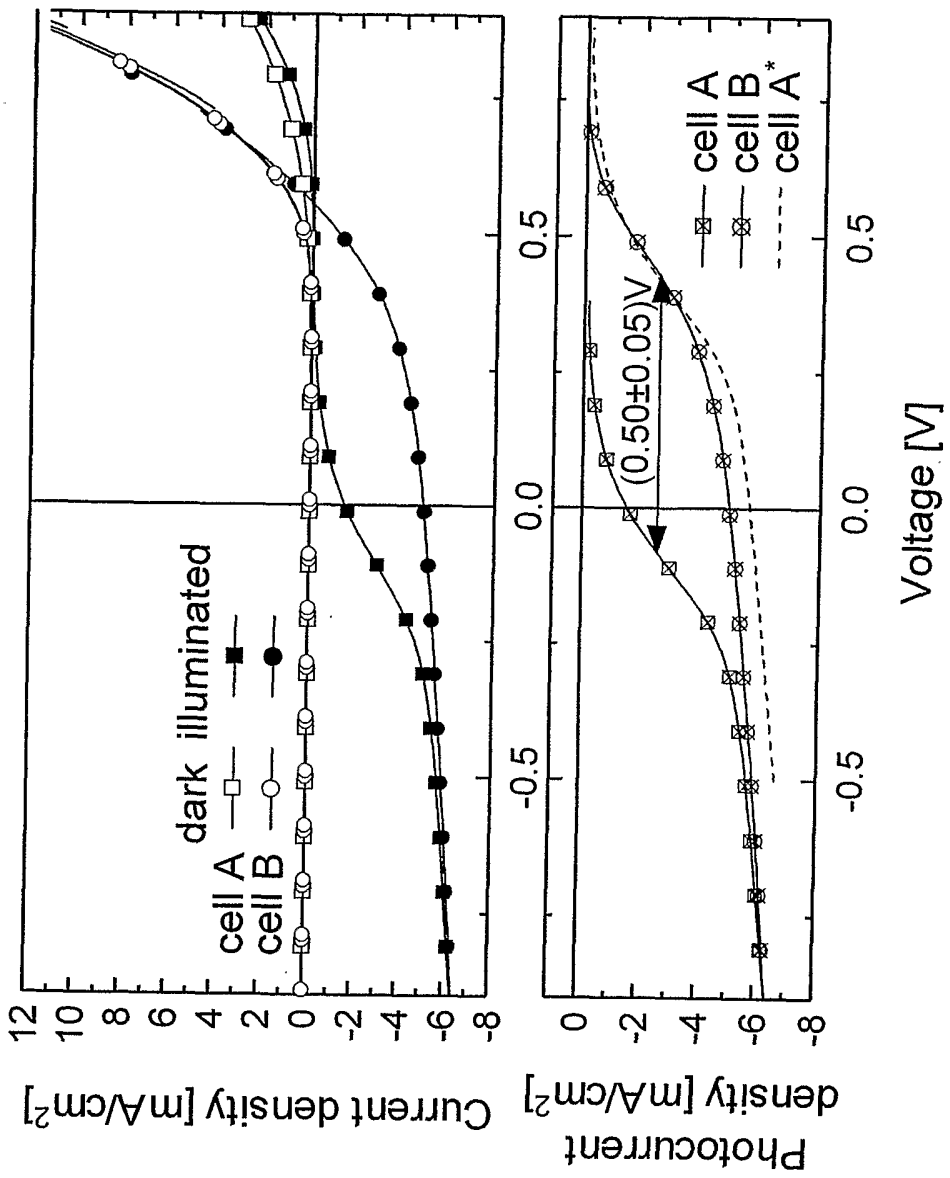
Current density [mA/cm²]
dark illuminated
cell A
cell B
12
10
8
6
4
2
0
-2
-4
-6
-8
Photocurrent density [mA/cm²]
(0.50±0.05)V
cell A
cell B*
cell A*
0
-2
-4
-6
-8
-0.5
0.0
0.5
Voltage [V]

Figure 12

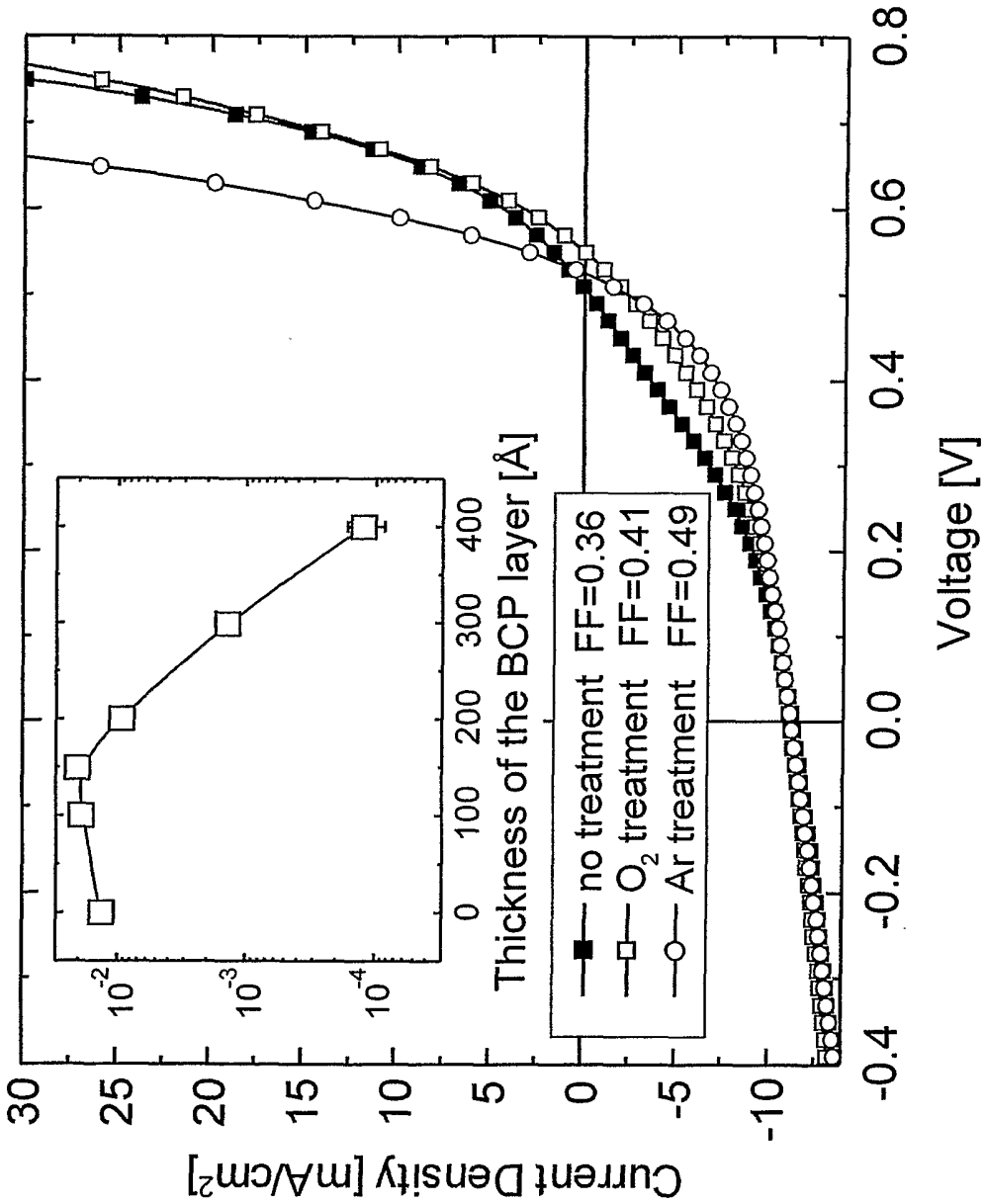
Current Density [mA/cm²]
Voltage [V]
30
25
20
15
10
5
0
-5
-10
-0.4
-0.2
0.0
0.2
0.4
0.6
0.8
no treatment FF=0.36
O2 treatment FF=0.41
Ar treatment FF=0.49
Thickness of the BCP layer [Å]
0
100
200
300
400
10-2
10-3
10-4

Figure 13

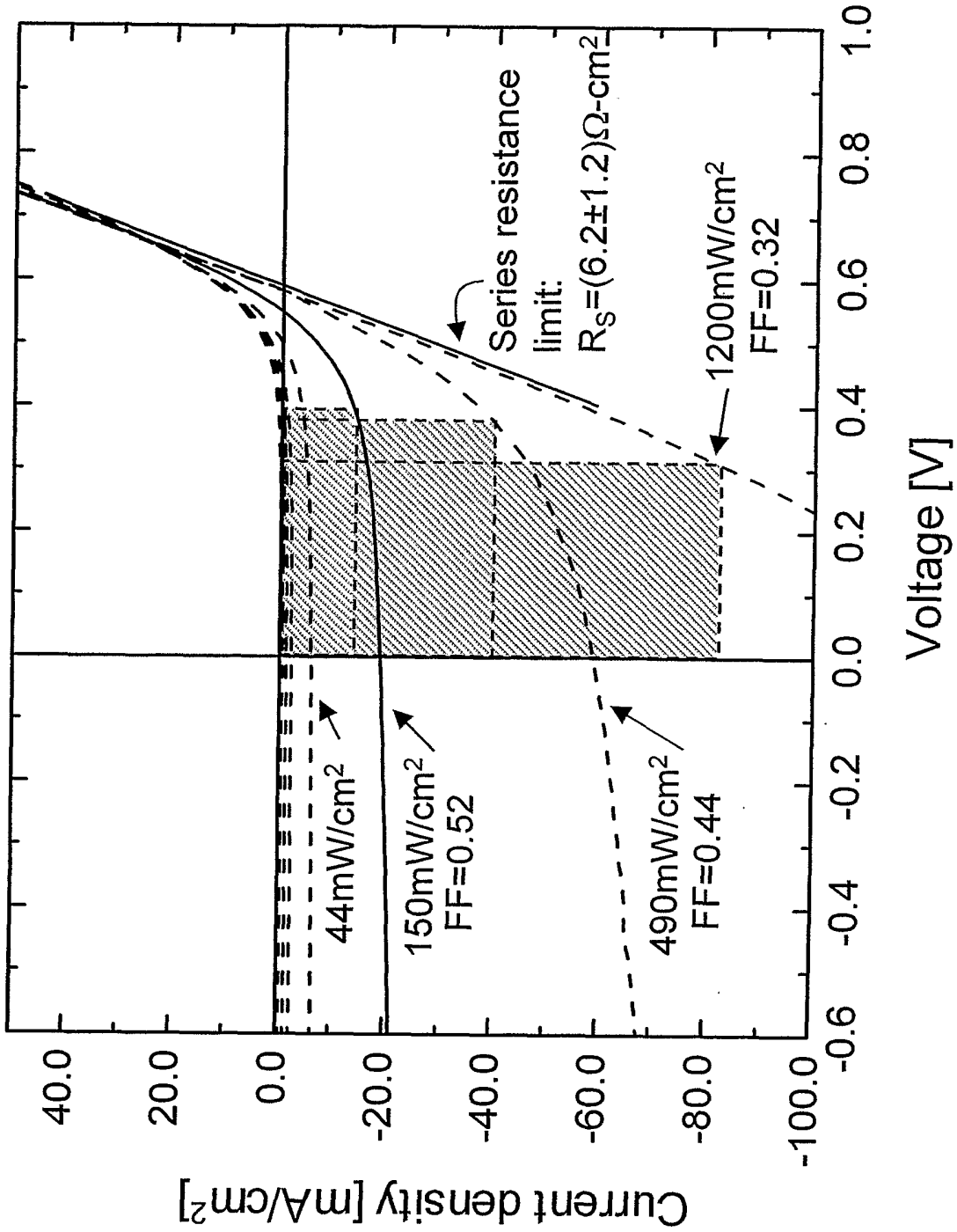
Current density [mA/cm2]
40.0
20.0
0.0
-20.0
-40.0
-60.0
-80.0
-100.0
-0.6
-0.4
-0.2
0.0
0.2
0.4
0.6
0.8
1.0
Voltage [V]
Series resistance limit:
Rs=(6.2±1.2)Ω-cm2
1200mW/cm2
FF=0.32
44mW/cm2
150mW/cm2
FF=0.52
490mW/cm2
FF=0.44

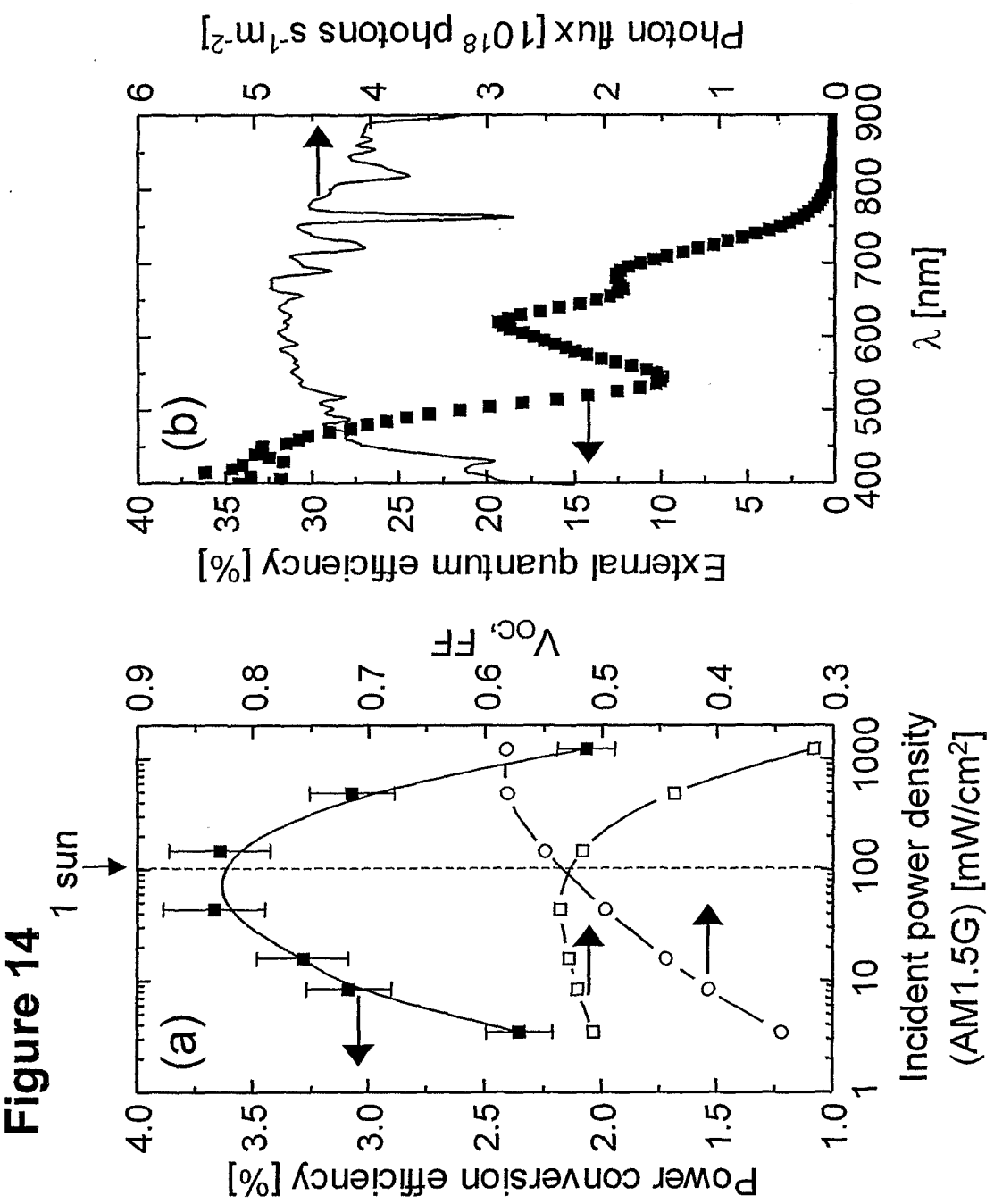
Photon flux [10^18 photons s^-1m^-2]
External quantum efficiency [%]
(b)
λ [nm]
Power conversion efficiency [%]
(a)
1 sun
Voc, FF
Incident power density
(AM1.5G) [mW/cm^2]

Figure 14

INTERNATIONAL SEARCH REPORT

International application No.
PCT/US02/18183

A. CLASSIFICATION OF SUBJECT MATTER

IPC(7) : H01L 31/0256, 31/04, 31/06
US CL : 136/263, 255, 256, 252; 257/40, 431, 443, 461; 438/82, 73, 74

According to International Patent Classification (IPC) or to both national classification and IPC

B. FIELDS SEARCHED

Minimum documentation searched (classification system followed by classification symbols)
U.S. : 136/263, 255, 256, 252; 257/40, 431, 443, 461; 438/82, 73, 74

Documentation searched other than minimum documentation to the extent that such documents are included in the fields searched

Electronic data base consulted during the international search (name of data base and, where practicable, search terms used)

C. DOCUMENTS CONSIDERED TO BE RELEVANT

Category *	Citation of document, with indication, where appropriate, of the relevant passages	Relevant to claim No.
X --- Y	WO 00/11725 A1 (FORREST et al) 02 March 2000 (02.03.2000), pages 33-37 and 44.	1, 5, 7-15, 18, 35 ---------- 2-4, 6, 16, 17, 19-34, 36-39
Y	PEUMANS et al. Efficient photon harvesting at high optical intensities in ultrathin organic double-heterostructure photovoltaic diodes. Applied Physics Letters. 08 May 2000, Vol. 76, No. 19, pages 2650-2652, especially page 2650.	2-4, 6, 16, 17, 19-34, 36-39
Y	PETTERSSON et al. Modeling photocurrent action spectra of photovoltaic devices based on organic thin films. Journal of Applied Physics. 01 July 1999, Vol. 86, No. 1, pages 487-496, especially page 488.	6, 24, 25
Y,P	US 6,333,458 B1 (FORREST et al) 25 December 2001 (25.12.2001), figure 2A.	33, 34

☐ Further documents are listed in the continuation of Box C. ☐ See patent family annex.

* Special categories of cited documents:

"A" document defining the general state of the art which is not considered to be of particular relevance

"E" earlier application or patent published on or after the international filing date

"L" document which may throw doubts on priority claim(s) or which is cited to establish the publication date of another citation or other special reason (as specified)

"O" document referring to an oral disclosure, use, exhibition or other means

"P" document published prior to the international filing date but later than the priority date claimed

"T" later document published after the international filing date or priority date and not in conflict with the application but cited to understand the principle or theory underlying the invention

"X" document of particular relevance; the claimed invention cannot be considered novel or cannot be considered to involve an inventive step when the document is taken alone

"Y" document of particular relevance; the claimed invention cannot be considered to involve an inventive step when the document is combined with one or more other such documents, such combination being obvious to a person skilled in the art

"&" document member of the same patent family

Date of the actual completion of the international search
09 September 2002 (09.09.2002)

Date of mailing of the international search report
27 SEP 2002

Name and mailing address of the ISA/US
Commissioner of Patents and Trademarks
Box PCT
Washington, D.C. 20231
Facsimile No. (703)305-3230

Authorized officer
Alan Diamond

Telephone No. 703-308-0661

Form PCT/ISA/210 (second sheet) (July 1998)